Title: A Massively Parallel CRISPR-Based Screening Platform for Modifiers of Neuronal Activity

Authors: Steven C. Boggess[1,2], Vaidehi Gandhi[1,2], Ming-Chi Tsai[4], Joanna Yu-Ying Chou[1,2,3], Xiaoyu Hu[6], Lin Yadanar, [1,2], Noam Teyssier,[1,2,5] Celine Eidenschenk[6], Jesse E. Hanson[4], Ruilin Tian[1,2], Martin Kampmann[1,2,7,8].

1. Institute for Neurodegenerative Diseases, University of California, San Francisco, San Francisco, CA, USA
2. Weill Institute for Neurosciences, University of California, San Francisco, San Francisco, CA, USA
3. City College of San Francisco, San Francisco, CA, USA.
4. Department of Neuroscience, Genentech, South San Francisco, CA, USA
5. Biological and Medical Informatics Graduate Program, University of California, San Francisco, San Francisco, CA, USA
6. Department of Functional Genomics, Genentech, South San Francisco, CA, USA
7. Department of Biochemistry and Biophysics, University of California, San Francisco, San Francisco, CA, USA
8. Correspondence: martin.kampmann@ucsf.edu

Abstract:

Understanding the complex interplay between gene expression and neuronal activity is crucial for unraveling the molecular mechanisms underlying cognitive function and neurological disorders. In this study, we develop pooled screens for neuronal activity, using CRISPR interference (CRISPRi) and the fluorescent calcium integrator CaMPARI2. Using this screening method, we identified 153 genes associated that changed synaptic excitability in human iPSC-derived neurons, revealing potential links to neurodegenerative and neurodevelopmental disorders. These genes include known regulators of neuronal excitability, such as TARPs and ion channels, as well as genes associated with autism spectrum disorder (ASD) and Alzheimer's disease (AD) not previously described to affect neuronal excitability. This CRISPRi-based screening platform offers a versatile tool to uncover molecular mechanisms controlling neuronal activity in health and disease.

Introduction

Billions of neurons in the human brain form a complex, dynamic network that gives rise to the emergent properties of cognition, memory, and behavior. Different neuronal cell types in the brain are defined by distinct patterns of gene expression and have unique intrinsic and synaptic properties that drive well-defined patterns of neuronal activity. Neuronal activity, in turn, further alters gene expression to affect the composition of synaptic receptors and ion channels at the neuronal membrane, allowing for plasticity and homeostatic control of individual neurons and circuits. Large-scale efforts to map gene expression to different areas of the brain,[1,2] at single cell resolution[3,4], or to connect transcriptional changes to electrophysiological measurements[5] are underway, but we lack a systematic understanding of how expression differences of individual genes affect neuronal activity.

One approach to link genes to neuronal activity and brain function is to map genetic risk factors underlying neurological disorders that are characterized by neuronal activity changes. In epilepsy, human genetics have revealed mutations in voltage-gated ion channels (channelopathies), synaptic channels (synaptopathies), and metabolic genes in both sporadic[6] and familial[7] disease. Other diseases, such as Alzheimer's Disease (AD) and autism spectrum disorder, also involve changes in neuronal activity. However, it is unclear which of the associated risk genes[8,9] affect neuronal activity, and we lack a systematic and scalable approach to establish the effect of genes on neuronal function.

Classically, interrogation of neuronal activity mechanisms has been accomplished through patch-clamp electrophysiology. This technique is the gold-standard to measure a range of properties, including spontaneous synaptic currents and individual channel kinetics. While powerful, these techniques are limited by the number of neurons that can be interrogated as the researcher must make physical contact with each individual neuron. This requires both a high degree of technical skill and large time investment to evaluate each perturbation.

To measure electrical activity from dozens of neurons in a network simultaneously, researchers have turned to the use of multi-electrode arrays (MEAs) and fluorescent activity probes. MEAs circumvent some of the drawbacks of patch-clamp electrophysiology by measuring local field potentials in a network of neurons but are costly and often sacrifice single-neuron spatial resolution. Alternatively, fluorescence-based indicators of calcium[10] and membrane potential[11,12] also circumvent the throughput constraints of patch-clamp electrophysiology while still providing single-neuron resolution. Furthermore, optogenetics using microbial-opsins provides additional temporal control and the ability to stimulate specific neurons.[13,14] Still, the number of perturbations, genetic or pharmacologic, that can be performed are limited in that each must be done in an arrayed format on high-content imaging plates. Recently, it was shown that calcium oscillations detected using GCaMP6 could be used for multiparametric drug screening in healthy and $SOD1^{A4V}$ motor-neurons differentiated from human iPSCs,[15] however, to our knowledge, a method capable of

comprehensively evaluate genetic modifiers of activity on a genome-wide scale has not been reported.

To enable the scalable characterization of gene function in human cells, we developed CRISPR interference (CRISPRi) and activation (CRISPRa) screening[16] and implemented it in human iPSC-derived cell types relevant for brain function and diseases, including neurons,[17,18] microglia,[19] and astrocytes.[20] These screens allow for unbiased identification of genes and mechanisms underlying cell type specific biological processes. Pooled CRISPR-based screens have been successfully deployed to elucidate neuronal phenotypes such as survival,[17,18,21] transcriptomic states,[17,18] oxidative damage,[18] lysosomal function,[18] and protein aggregation,[22] it has so far not been possible to use pooled CRISPR-based screens to uncover modifiers of neuronal activity. Here, we report a method to uncover modifiers of neuronal excitability in massively parallel screens.

To overcome the challenges in evaluating modifiers of neuronal activity at scale, we developed a pooled screening approach using integration of calcium signal. The fluorescent calcium integrator CaMPARI2 acts as an irreversible record of calcium levels in a neuron by photoconverting while in the presence of high calcium and UV light.[23–26] Based on the ratio of photoconversion in each neuron, the relative level of activity can be discerned by flow cytometry. Using this tool in conjunction with CRISPRi, we conducted pooled genetic screens and uncovered modifiers of neuronal excitability. We validated hit genes using calcium imaging and patch-clamp methods and generated hypotheses for how these hit genes regulate neuronal excitability.

Results

CaMPARI2 photoconversion provides a ratiometric readout for glutamate-induced activity in human iPSC-derived neurons

To establish a readout of neuronal activity compatible with pooled CRISPR-based screens using fluorescence-activated cell sorting (FACS), we evaluated the utility of the fluorescent calcium integrator CaMPARI2.[26] We introduced a CaMPARI2 transgene into our iPSC line expressing CRISPRi machinery and inducible Ngn2[17] using lentiviral integration followed by clonal selection (Figure 1a). These iPSCs are rapidly differentiated into glutamatergic neurons by doxycycline-induced expression of NGN2, and express dCas9-KRAB for efficient knockdown of genes targeted by a sgRNA.[17]

Synaptic dysfunction is a critical hallmark of many human neurological diseases,[27–31] therefore we focused our efforts on establishing a CaMPARI2-readout for synaptic excitability. To depolarize glutamatergic synapses, we stimulated iPSC-neurons with glutamate after 21 days of differentiation and illuminated with UV light to photoconvert CaMPARI2. We then measured the CaMPARI2 red-to-green fluorescence ratio after glutamate stimulation using both microscopy and flow cytometry (Figure 1b). With confocal microscopy, we found a robust increase in CaMPARI2 photoconversion in neurons treated with glutamate compared to vehicle control (Figure 1c). Virtually no

photoconversion was observed with glutamate treatment in tetrodotoxin (TTX)-treated neurons (Figure 1c). TTX-treated neurons showed similar signal compared to vehicle control suggesting that the baseline synaptic excitability of iPSC-neuron cultures is low.

We tested the dose-response relationship of glutamate and CaMPARI2 photoconversion by flow cytometry (Figure 1d) and found that incubation with 30 µM glutamate for 5 minutes followed by exposure to UV light provided good signal without reaching saturation. This intermediate concentration was chosen to provide dynamic range to enable identification of genetic modifiers that either decrease or increase excitability. Furthermore, we found that 5 minutes of UV illumination maximized signal with minimal cell death during the experimental timeline (Extended Data Figure 1). We also found that neuron plating density had little effect on the photoconversion outcome and that 21 days of differentiation was sufficient to generate adequate signal. Co-incubation of APV and NBQX, antagonists for NMDA and AMPA receptors, with glutamate demonstrates the detected calcium release is primarily through AMPA receptors (Figure 1e).

CRISPRi screen for modifiers of neuronal excitability

With this technology in hand, we focused our efforts to study neuronal excitability, which has been implicated in many neurological disorders. Patients with Alzheimer's Disease (AD) have an 8- to 10- fold increase in the risk of seizures,[32,33] with familial early-onset cases having more severe risk,[32] and seizure prevalence has been associated with accelerated cognitive decline.[34] Furthermore, neuronal network dysfunction has been proposed as a critical contributor to AD that occurs decades before clinical symptoms manifest.[35] Epilepsy also shows comorbidity with 5-46% of individuals with autism spectrum disorder (ASD),[31] which is believed to be caused by an imbalance of synaptic excitation and inhibition (E/I balance) or dysfunctional ion channels. Identifying the genetic etiology can help inform precise treatment options for patients;[7,36] however, many of these cases are resistant to current anti-seizure medications and monogenic syndromes are only identified in about 40% of patients with epilepsy.[7] This highlights the need for methods that comprehensively evaluate the functional consequences of genetics on neuronal activity.

To establish CRISPRi screening based on the CaMPARI2 reporter, we generated a custom sgRNA library targeting 1,343 genes selected based on their known or proposed roles in neuronal activity (Supplementary Data Table 1), neurodegeneration, and neurodevelopmental disorders (Supplementary Data Table 2). We designed this library to evaluate our screening paradigm by knocking down known regulators of neuronal excitability and potentially uncover new roles for genes implicated in human diseases. The library targets each gene with 5 independent sgRNAs and contains 250 non-targeting control sgRNAs, resulting in a library of 7,450 different sgRNAs (Supplementary Data Table 3).

We transduced our CaMPARI2-CRISPRi-Ngn2 iPSCs with the lentiviral sgRNA library, selected for transduced iPSCs using puromycin, expanded, and then differentiated into neurons by inducing NGN2 expression with doxycycline (Figure 2a). After 21 days of differentiation, we stimulated neuronal activity with 30 µM glutamate, photoconverted CaMPARI2 with UV light for five minutes using a UV light box, and then dissociated neuronal cultures for FACS. We collected neurons with the highest 35% and lowest 35% CaMPARI2 red/green fluorescence ratio. We determined the frequency of neurons expressing each sgRNA in the library using next-generation sequencing to determine which sgRNAs cause significant increase or decrease in CaMPARI2 response to glutamate exposure (Figure 2a). We performed this screen in duplicate to identify the most robust hits.

Of the 1,343 genes targeted by our custom sgRNA library, we identified 116 genes for which knockdown decreased synaptic excitability and 37 genes for which knockdown increased synaptic excitability, for a total of 153 hits (Figure 2b, FDR 0.1). We found that the observed hits have Gene Ontology (GO) annotations related to neurotransmitter receptor activity, ion transport, and synaptic transmission (Extended Data Figure 2a).

We performed an Over-Representation Analysis (ORA) using WebGestalt[37] to identify enrichment of functional classes of genes among the hits (Figure 2b,c). Of the hits that increased synaptic excitability, GO terms for membrane protein localization, clathrin coat assembly, and negative regulation on ion transmembrane transport were over-represented, potentially highlighting mechanisms related to neuronal homeostasis at the plasma membrane and synaptic vesicle recycling. Additionally, many GO terms related to gene transcription and chromatin regulation (Figure 2c) were over-represented in hits that decrease synaptic excitability, which suggests altered gene expression is important for synaptic function or could be related to delayed neuronal differentiation. The GO term *Cellular Response to Amino Acid Starvation*, an arm of the integrated stress pathway (ISR), was over-represented in hits decreasing synaptic excitability. Previous studies have explored the use of ISRIB, and ISR inhibitor, to restore cognitive deficits in mice.[38] Furthermore, our screen revealed that knockdown of *EIF2AK3, EIF2AK4,* and *ATF4* reduced excitability, in line with previous work showing the role of eIF2α in long-term memory formation.[39,40] These hit genes highlight that neuronal excitability is influenced by diverse molecular pathways and that the CaMPARI2-based screening method is capable of detecting neuronal excitability modifiers that are upstream in these pathways.

Many hit genes have been associated with Alzheimer's Disease, epilepsy, and/or autism spectrum disorder (Figure 2d, Extended Data Figure 2b). While our custom library was purposely enriched with these disease-associated genes (Supplementary Data Table 2), this screen suggests a potential, previously unknown role these hit genes play in regulating neuronal excitability.

Validation of screen hits reveals mechanisms of altered excitability including altered synaptic function and action potential dynamics

We examined these observed screen phenotypes by flow cytometry using two individual guides targeting *CACNG2* and *KCNT2*, directly comparing the CaMPARI2 ratio after glutamate stimulation of iPSC-neurons receiving the sgRNA versus iPSC-neurons without guide (Figure 3a). This is expressed as a normalized CaMPARI ratio (neuronal excitability), where the mean response of neurons in wells with no sgRNA transduction is equal to one. We evaluated neuronal networks in which 100% of neurons received a sgRNA and networks in which 50% of neurons received a sgRNA which allowed us to evaluate both cell autonomous and cell non-autonomous effects on neuronal excitability.

Knockdown of *CACNG2* decreased neuronal excitability in response to glutamate when compared to neurons that were not transduced with the sgRNA (Figure 3a). We tested the effect of this knockdown in neuronal populations where approximately 50% of the neurons expressed an sgRNA and found a robust decrease in excitability in *CACNG2* knockdown neurons compared to intra-well neurons without a sgRNA. In populations where approximately 100% of the neurons had *CACNG2* knockdown, neuronal excitability was dramatically reduced when compared to populations of neurons without sgRNA treatment (Figure 3a). Similarly, with *KCNT2* knockdown we observed increased excitability as observed in the screen (Figure 3a). In populations where all neurons were transduced, there was an overall decrease in excitability, which opposes the screen phenotype and suggests more complicated roles for *KCNT2* via both cell autonomous and network level impacts. Together, these results suggest that the CaMPARI2 screening modality can capture genetic modifiers of activity.

Our CaMPARI2-based CRISPRi screening method positively identified modifiers of neuronal excitability, including AMPAR (*CACNG2, GRIA4*) and NMDAR (*GRIN2A*, *GRIN2B*) subunits and ion channels (*KCNT2, CACNA1C, CACNA1D*). To explore neuronal excitability mechanisms that could be detected by the CaMPARI2 screening approach, we evaluated the effects of *CACNG2* and *KCNT2* perturbation using whole-cell electrophysiology. For these experiments, ribonucleoprotein (RNP) mediated CRISPR was used to generate knockouts (KOs) in human iPSC neurons, with NTC guides as negative controls. Recordings of spontaneous excitatory postsynaptic currents (sEPSCs) revealed differences in synaptic activation between *CACNG2* KO neurons and neurons treated with NTCs (Figure 3b). A small reduction in the frequency of detected sEPSCs in *CACNG2* KOs was observed compared to NTC (Figure 3c). Furthermore, the half-width and charge transfer of these sEPSCs was significantly attenuated in *CACNG2* KO neurons (Figure 3d-e), reflecting altered receptor kinetics. This decreased synaptic activation observed in the whole cell recordings aligns with previous observations,[41–46] and reflects the reduced excitability observed in the CaMPARI2 screen. These results indicate that the CaMPARI2 screening approach is sensitive to detect known regulators of synaptic excitability with complex electrophysiological phenotypes.

We observed no effect on passive membrane properties in *KCNT2* KO neurons. However, large current injections caused a drop in action potential firing rate in *KCNT2* KO neurons and premature entry into depolarization block, whereas neurons with a NTC sgRNA do not (Figure 3f-g). This depolarization block may lead to sustained activation of Ca^{2+} channels and lead to an increase in CaMPARI2 signal in our screen and flow cytometry experiments with 50% of neurons with *KCNT2* KD. At the same time, in cultures with 100% of neurons with *KCNT2* KO/KD, the reduced numbers of action potentials could lead to reduced network activity which may have a dominant effect in reducing overall excitability that overrides the cell-autonomous increases in calcium influx. This would lead to the decrease in CaMPARI signal we observed by flow cytometry in cultures where 100% of neurons have *KCNT2* KD. Others have postulated a potential protective role for $K_{Na}1.2$ in the acute phase of traumatic brain injury (TBI), based on an increase in $K_{Na}1.2$ expression surrounding TBI lesions in the acute phase following TBI in mice with increased neuronal excitability, and seizure susceptibility in *KCNT2* $^{-/-}$ mice compared to WT.[47] These results demonstrate that the CaMPARI2 screen is capable of detecting subtle changes to neuronal excitability and can highlight previously under-studied channels for additional characterization.

Modifiers identified in the CaMPARI2 screen are reproducible, specific to neurons, and can be stimulus-specific

We generated a focused CRISPRi sgRNA library targeting 395 hit genes (Supplementary Table 4) from our primary screen (based on a relaxed criterion for hit genes, see Methods) for secondary validation screens. We subjected CaMPARI2 neurons to either treatment with 30 µM glutamate or 50 mM KCl in two independent screens (Figure 4a). We selected 50 mM KCl treatment as it resulted a CaMPARI2 response with large dynamic range. Furthermore, we collected neurons at the start of differentiation (day 0) and after 21 days of differentiation (before stimulation and photoconversion) to identify knockdowns that affect neuronal survival (Figure 4b). To assess which hit genes are specific to glutamate-stimulated activity in neurons, rather than affecting the CaMPARI2 signal via effects on general cellular calcium homeostasis, we also treated a subset of the sgRNA-transduced undifferentiated iPSCs with glutamate and used the same photoconversion and FACS strategy (Figure 4c).

Comparison of gene scores from our primary glutamate-based screen (Figure 2) and our secondary glutamate-based validation screen showed a high degree of correlation (Pearson's R = 0.60, Figure 4d), suggesting that the CAMPARI2 screening paradigm produces reproducible results. Many genes had similar effects when knocked down in the secondary glutamate-stimulated screen and the KCl-stimulated screen (Pearson's R = 0.33, Figure 3e), suggesting mechanisms that modify neuronal excitability in a general way irrespective of the depolarization method. Still, there are many hits that specifically modify excitability in the glutamate screens, but not in the KCl screen, indicating mechanisms specific to glutamate-receptor stimulation and/or different sensitivities of the screens. For instance, *KCNT2* KD had no significant phenotype with KCl-mediated

depolarization, despite our observation that *KCNT2* KO neurons enter depolarization block prematurely during high levels of current injection (Figure 3f-g).

In the survival screen, we found 90 significant hit genes that show a toxic knockdown phenotype in neurons, with 16 protective hits. Comparison to the secondary glutamate screen (Figure 4f) shows little correlation of these effects (Pearson's R = 0.064). Furthermore, we did not identify any significant hits in iPSCs treated with glutamate (Figure 4g). Together, these results indicate that the CaMPARI2 screen is specific in detecting modifiers of neuronal excitability.

Evaluating mechanisms of disease-associated modifiers of excitability

We selected six additional hit genes that have been associated with human neurological disease for additional validation (Figure 5). *NSD1* and *PHF21A*, both of which decreased synaptic excitability in the glutamate screens, are histone modifiers that have been identified as risk genes for ASD. Comparing the CaMPARI2 response in neurons receiving sgRNAs normalized to neurons without a guide, individual KD of *NSD1* and *PHF21A* recapitulated the observed phenotype in the screen (Figure 5a). We also validated the screening phenotype for *GRIA2* (Figure 5a), an AMPA receptor subunit that is downregulated after kainite-induced status epilepticus in the hippocampus.[48,49]

We then examined three hits that increased neuronal excitability in the CaMPARI2 CRISPRi screens. *CACNG7* encodes γ-7, which is related to stargazing, has been found to be reduced in mouse models of spinocerebellar ataxia type 23 (SCA24).[50] In the screen, *CACNG7* KD increased neuronal excitability and we observe a general increase in neuronal excitability in *CACNG7* KD neurons in independent experiments (Figure 5b). *PTEN*, classically associated with its role as a tumor suppressor gene[51] and in mitophagy,[52] has been shown to modulate neurite outgrowth and synapse density in *PTEN* KO mice.[53] Furthermore, recent whole-exome sequencing studies have implicated *PTEN* in ASD.[9] In the CaMPARI2 screen, *PTEN* KD increased synaptic excitability and *PTEN* KD neurons are more excitable when compared to baseline neurons (Figure 5b).

Recently, it has been suggested that *PICALM* may also regulate calcium permeable (CP)-AMPA receptors (AMPARs with homomeric GluA1 subunits) by targeting surface receptors for endocytosis.[54] To test for regulation of CP-AMPARs in human iPSC-neurons, we performed patch clamp recordings in *PICALM* KO and non-targeting control iPSC-neurons. In these experiments we measured AMPA receptor mediated sESPC amplitudes at depolarized and hyperpolarized holding potentials and calculated the rectification index ($sESPC_{AMPAR}$ +40 mV / $sESPC_{AMPAR}$ -70 mV). While a high rectification index indicates few CP-AMPARs, a low rectification index indicates the presence of CP-AMPARs. We found a decrease in the rectification index in *PICALM* KO iPSC-neurons compared to non-targeting control (Figure 6), suggesting that

PICALM KO increases the level of CP homomeric GluA1 AMPARs at the synapses of human iPSC-derived neurons.

Discussion

Changes in neuronal excitability and synaptic dysfunction appear in many neurodegenerative[27,34,55–57] and neurodevelopmental[28,31,58] disorders. In this work, we developed a screening paradigm using calcium integration as a proxy for neuronal activity to explore how perturbation of genes known to regulate to neuronal activity and/or identified risk genes affect synaptic excitability of iPSC-neurons. We found that we could detect the effect of glutamate receptor subunits, TARPs, and ion channels. These hits were confirmed with patch clamp studies and suggests that mechanisms such as altered depolarization-induced action potential dynamics, altered synaptic receptor kinetics, and changes in AMPA receptor calcium permeability could underlie the observed screen phenotypes. The screens and validation experiment also confirmed that roles in neuronal excitability for disease-linked genes could be detected with this approach.

The CaMPARI2 screen evaluated the effect of known modifiers of synaptic excitability in iPSC-neurons. Multiple genes belonging to the transmembrane AMPA receptor protein (TARP) family were identified as hits. TARPs are known to influence the density and function of AMPARs.[41,46] The type-I TARP encoded by *CACNG2* has previously been shown to interact with PSD-95 to stabilize AMPARs at the postsynaptic density[43] and to modulate AMPA receptor levels [42,46] and kinetics.[46] Of the six known TARP isoforms,[42] CRISPRi knockdown of *CACNG2* and *CACNG4* reduced synaptic excitability while *CACNG7* knockdown increased synaptic activation in the CaMPARI2 based screen (Figure 2b). *KCNT2* encodes the sodium-activated potassium channel $K_{Na}1.2$ (Slick). Potassium (K^+) channels play a major role in modifying neuronal excitability and regulating synaptic vesicle release,[59] and $K_{Na}1.2$ has been implicated in the adaptation of neuronal firing patterns in auditory neurons.[60] Gain-of-function variants in the $K_{Na}1.1$ (Slack) channel encoded by *KCNT1*, a paralogue of *KCNT2*, have been extensively linked to neurodevelopmental disorders (NDD) and epilepsy;[61,62] however, the function of $K_{Na}1.2$ is less understood, despite the connection of $K_{Na}1.2$ variants to developmental and epileptic encephalopathy[63] and epilepsy.[64] Knockdown of *KCNT2* increased excitability in iPSC-neurons in the CaMPARI2 screen (Figure 2b).

Evaluating disease risk genes for their role in neuronal activity presents a oissbe route to developing new therapeutics. *PICALM* encodes the phosphatidylinositol-binding clathrin assembly protein (PICALM), and is originally noted for its involvement in AP2-dependent clathrin-mediated endocytosis.[65,66] GWAS studies have implicated variants at the *PICALM* locus to be associated with late-onset AD,[67,68] which has been verified with additional meta-analysis[69,70] and functionally shown to modify the clearance of tau.[71] We observed an increase in synaptic excitability with *PICALM* KD in the CaMPARI2 screen with glutamate, and PICALM KD increased excitability with the largest effect size of the genes tested in the individual validation experiments (Figure

5b). Other studies have noted late-onset AD risk genes, including *PICALM*, to be involved with synaptic dysfunction[27] and a recent study demonstrated the role of *PICALM* in the regulation of long-term potentiation and memory.[54]

To our knowledge, this calcium-integration strategy represents the first pooled modifier screen for neuronal activity. Intriguingly, this strategy uncovered modifiers of numerous aspects of neuronal excitability, including depolarization block, changes to receptor kinetics, and modifications to receptor subunit partitioning at the synapse. While these CRISPRi screens using CaMPARI2 can uncover potentially novel roles for genes in neuronal activity and excitability, we note there are limitations with this method. Primarily, the 405 nm (UV) light needed for CaMPARI2 photoconversion can cause photodamage to cells. We demonstrate that neurons exposed to the five minutes of 405 nm light used in the screen do not undergo massive death or enter apoptosis on the same timescale of the screen, however we acknowledge low cell recovery from FACS, which we attribute to the fragility of these neurons. We were able to overcome this obstacle because of the scalability of our iPSC-neuron system. However, screening the entire protein coding genome will be a major endeavor. To combat this drawback, we plan to incorporate other calcium integration strategies such as scFLARE.[72] This strategy uses 488 nm light to initiate activation through a conformational change of the sensor, which is less toxic than UV light. Furthermore, this Ca^{2+} integration strategy can be modified to provide a transcriptional readout,[73] which could be paired with CRISPRi for transcriptional perturbation screens using either the Perturb-seq or CROP-seq method.

Another potential drawback of our first application of this approach is the limited functional maturity of iPSC-neurons. We chose to perform these studies after 21 days of differentiation in BrainPhys media, which helps to accelerate maturation of iPSC-derived cultures,[74,75] as this provided a timepoint where the neurons displayed reasonable spontaneous activity while also convenient for screening. Generally, extended maturation times upwards of 9 weeks (>60 days) are needed to develop synaptic maturity in these iPSC-neuron systems[76] and co-culture with astrocytes is needed to enhance the maturation of iPSC-neurons and facilitate increases in activity.[77]

In the first application of this CaMPARI2-based pooled screen, we decided focus on synaptic excitability due to prevalence of synaptic defects in many neurological disorders. However, this screening approach could be adapted to examine neuronal activity in response to other pharmacologic agents like kainic acid to produce seizure-like firing. Furthermore, CaMPARI2 screens could be used to evaluate electrophysiological maturation of iPSC-neurons longitudinally or to probe mechanisms of plasticity. Optogenetic tools that are spectrally compatible with CaMPARI2 could be used in this paradigm to examine how particular genes affect specific firing partterns of neurons.

We believe that our CaMPARI2-based CRISPRi screening platform will help to uncover the functional roles of risk genes for many different neurological disorders of

both the central and peripheral nervous systems. The development of new differentiation protocols and increased availability of iPSC models provides an opportunity to extend this paradigm to other specialized types of neurons, such as motor neurons and inhibitory neurons, and to patient-derived iPSC-neurons with disease-linked mutations. Understanding the genetic determinants of neuronal activity in different contexts will lead to an understanding of disease mechanisms related to aberrant neuronal activity potential and the development of new therapeutics.

Methods

Human iPSC Culture

hiPSCs were cultured in StemFlex medium (Thermo Fisher Scientific, A3349401) in plates or dishes coated with Growth Factor Reduced, Phenol Red-Free, LDEV-Free Matrigel Basement Membrane Matrix (Corning, 356231) diluted 1:100 in Knockout DMEM (Thermo Fisher Scientific, 10829–018). StemFlex medium was replaced daily. Upon 70-80% confluence, hiPSCs were dissociated to single-cell suspensions with StemPro Accutase Cell Dissociation Reagent (Thermo Fisher Scientific, A1110501). hiPSCs were washed with Dulbecco′s Phosphate Buffered Saline without $CaCl_2$ and $MgCl_2$ (Sigma, D8537-24X500ML), incubated with Accutase for 3-7 minutes at 37°C until cell could be dislodged with gentle trituration. The cell suspension was diluted 5x with DPBS, transferred to tubes, and centrifuged at 200xg for 5 minutes. hiPSCs were resuspended in StemFlex Medium supplemented with 10 nM Y-27632 dihydrochloride ROCK inhibitor (Tocris Bioscience, 1254), counted, and plated onto Matrigel-coated plates or dishes. hiPSCs were maintained in Y-27632 until colonies reached the appropriate size (more than 15 cells/colony). Studies with human iPSCs at UCSF were approved by the Human Gamete, Embryo, and Stem Cell Research (GESCR) Committee. Informed consent was obtained from the human subjects when the hiPSC lines were originally derived.

Generation of CaMPARI2 hiPSC line

To generate CaMPARI2 iNeurons, the CaMPARI2 gene (1446 bp) was subcloned from pAAV_hsyn_NES-his-CaMPARI2-WPRE-SV40 (Addgene 101060, gift from Eric Schrieter)[26] into a lentiviral plasmid (pRT050) under a CAG promoter and an upstream UCOE element via Gibson Assembly to yield pRT074. iPSCs expressing CRISPRi machinery and inducible NGN2[17] were transduced with lentivirus delivering pRT074 (described in more detail below). Clonal lines were isolated by colony picking, differentiated to neurons, and evaluated for homogeneity of CaMPARI2 expression and dynamic range of photoconversion. A clonal line satisfying the above criteria was selected for CaMPARI2 photoconversion experiments and screening.

Lentiviral transduction of iPSCs

CaMPARI2 (pRT074)

pRT074 was lentivirally packaged in HEK 293T cells (ATCC Cat. No. CRL-3216) DMEM complete medium: DMEM (Gibco, 11965-092) supplemented with 10% FBS (VWR, 89510, lot: 184B19), 1% penicillin-streptomycin (Gibco, 15140122), and 1% GlutaMAX (Gibco, 35050061) as described previously,[17] using TransIT Lenti Transfection Reagent (Mirus Bio; Cat. No. MIR 6600) according to manufacturer's protocol.

sgRNA constructs

Individual or pooled sgRNAs were lentivirally packaged in HEK 293T cells (ATCC, CRL-3216) in DMEM complete medium as described previously[17] with the following modifications: a 3:1 ratio of 1 µg/µl polyethenylamine (PEI) (Linear, MW 25,000, Polysciences, 23966) to transfer DNA was used in place of TransIT Lenti Transfection Reagent. Cells were selected with 0.8 µg/mL puromycin (Gibco; Cat. No. A11138-03) for 2 days until the fraction of infected cells was > 0.95, as determined by flow cytometry of sgRNA-BFP fluorescence. Additional rounds of puromycin selection was used as necessary until the fraction of infected cells was above 0.95, after which cells were cultured for a single passage in the absence of puromycin to allow them to recover. sgRNA protospacer sequences are provided in Supplementary Table 7.

iNeuron differentiation and culture

For screening, flow cytometry, and imaging

hiPSCs were differentiated into iNeurons according to Tian et al.[17] At day 0 of differentiation, iNeurons were plated onto poly-D-lysine-coated plates (Corning 6W 356413, 12W 356470, 24W 354414, 96W 354640, 15cm 354550) in BrainPhys neuronal media (composed according to Bardy et al. 2015)[74] and 2 µg/ml doxycycline (Takara 631311). Three days after plating and, later, twice weekly, half of the culture media was removed and replenished with freshly supplemented BrainPhys without doxycycline. iNeurons were cultured for 21 days for all activity experiments.

For electrophysiology with RNP-CRISPR mediated knockouts (KO)

Human iPSCs from iP11N background (ALSTEM) with inducible expression of Ngn2 by doxycycline (Dox) were differentiated into neurons using combined Ngn2 programming and dual SMAD patterning according to optimized from a previously published protocol.[78] The iPSCs were cultured in mTeSR plus media for maintenance and in

initiation media (F12/DMEM media, N2, B27 without VA, glutamax, NEAA) for differentiation.

RNP-CRISPR knockouts

On day 7 of differentiation, cells were lifted by Accutase (Stemcell technology) and resuspended in P3 buffer (Lonza). RNP were prepared by mixing Cas9 (Alt-R™ S.p. Cas9 Nuclease V3, IDT) and gRNA for *KCNT2*, *CACNG2*, *PICALM* (Synthego KO kit) and non-targeting control (NTC) sequences (Genentech) separately. KO kits were used as a pool of three sgRNAs/gene (protospacer sequences are provided in Supplementary Table 6). These were then incubated at room temperature for 20 min. iNeurons in P3 buffer were then mixed with Cas9 RNP and nucleofected using pulse program CV-110 in the 4D-Nucleofector (Lonza). After nucleofection, iNeurons were plated at 1M in poly-D-lysine (A38904-01, Gibco) and iMatrix (T304, TaKaRa) coated µ-dishes (Cat. No. 80136, ibidi) for electrophysiology and further cultured in neuron maturation medium (iCell Neural Base medium 1 CDI M1010, iCell Neural Supplement B CDI M1029, iCell Nervous system Supplement CDI M1031) for more than 14 days before electrophysiology measurements were made.

iNeuron dissociation protocol for flow cytometry

Dissociation solution was made from resuspending papain (Worthington; Code: PAP2; Cat. No.LK003178) in 1X Hank's Balanced Salt Solution (Corning; Cat. No. 21-022-CV) to 20 U/mL. 5 mM $MgCl_2$ and 10 U/mL DNaseI (Worthington; Code: DPRF; Cat. No. LS006333) were then added to the solution. Dissociating solution was added to 96-well, 24-well, 12-well, 6-well plates and 15 cm dishes at volumes of 20 µL, 100 µL, 250 µL, 500 µL, and 5 mL, respectively. iNeurons were treated with dissociation solution for 12 minutes at 37ºC and resuspended in 1X Hank's Balanced Salt Solution (HBSS, Gibco) before analysis.

CaMPARI2 photoconversion

CaMPARI2 iNeurons plated on poly-D-lysine coated cell culture plates were illuminated with 405 nm light (LED output 39 W) in a temperature-controlled box with rotating turntable (FormLabs FH-CU-01). After 5 minutes of illumination at 37ºC, iNeurons were dissociated (see above) or imaged.

For imaging CaMPARI2 photoconversion, CaMPARI2 iNeurons were plated onto 96-well poly-D-lysine coated plates (Corning 354640) at 25,000 cells/well (78,000 cells/cm^2) in BrainPhys neuronal media. On day 21, iNeurons were treated with 30 µM

glutamate, 1.5 mM tetrodotoxin, or 0.1% DMSO (Vehicle) for 5 minutes at 37 ºC. After photoconversion (see above), iNeurons were imaged on an ImageXpress Micro Confocal High-Content Imaging System (Molecular Devices) using an Apo LWD 20X/0.95NA water immersion objective. Laser settings: Hoechst 33342 - EX 405/20 nm, EM 452/45 nm with FF409-Di03 dichroic; CaMPARI2-green - EX 467/21 nm; EM 520/40 nm with ZT 405/470/555/640/730 dichroic; CaMPARI2-red – EX 555 nm, EM 598/40 nm with ZT 405/470/555/640/730 dichroic.

CaMPARI2 photoconversion experiments for flow cytometry

CaMPARI2 iNeurons were plated onto 96-well poly-D-lysine coated plates (Corning 354640) at 25,000 cells/well (78,000 cells/cm^2) in BrainPhys neuronal media. On day 21, iNeurons were treated with 30 µM glutamate, 1.5 mM tetrodotoxin, or 0.1% DMSO for 5 minutes at 37 ºC. iNeurons were then photoconverted with UV light and dissociated as described above before analyzing them by flow cytometry using a BD LSRFortessa X14 (BD Biosciences) using BD FACSDiva (v.8.0.1.1) software. Flow cytometry data was analyzed using FlowJo analysis software (v10.10.0; BD Life Sciences; Ashland, OR, USA), R/G ratio was calculated for each event captured as the ratio of FITC and mCherry. Mean R/G was calculated for subsequent analyses of CaMPARI2 photoconversion.

Toxicity assays

CaMPARI2 cells at Day 0 of differentiation were plated in triplicate at 80,000 cells per well onto 24-well (42k cells/cm^2) poly-D-lysine-coated cellware (Corning 354414) in 400 µl/well of supplemented BrainPhys media. After 21 days of differentiation, CaMPARI iNeurons were UV illuminated for 0, 1, 5, 15, and 60 minutes. Viability was analyzed immediately after and 24 hours after UV exposure. CaMPARI2 iNeurons were dissociated as above, pelleted at 300xg for 5 minutes, and resuspended in 20 µl 1X HBSS, combined with 20 µL 0.4% Trypan Blue (Invitrogen T10282), and counted on a Countess II automated cell counter (Invitrogen AMQAX1000) to quantify viable cells.

CaMPARI2 iNeurons were plated onto 96-well poly-D-lysine coated plates (Corning 354640) at 25,000 cells/well (78,000 cells/cm^2) in BrainPhys neuronal media. On day 21, these were illuminated with UV for 0, 1, 5, 15, or 30 minutes. To perform viability staining with TO-PRO-3 (ThermoFisher T3605), CaMPARI2 iNeurons were washed 3x with DPBS, stained with TO-PRO-3 diluted 1:1000 in DPBS and 1 µM Hoechst 33342 (Thermo Fisher 62249) nuclear counterstain for 30 minutes at room temperature. After staining, cells were washed 3x with DPBS and imaged on an ImageXpress Micro Confocal High-Content Imaging System (Molecular Devices) using an Apo LWD 20X/0.95NA water immersion objective. Laser settings: TO-PRO-3; EX 638/17 nm, EM 624/40 nm with ZT 405/470/555/640/730 dichroic; Hoechst 33342; EX 405/20 nm, EM

452/45 nm with FF409-Di03 dichroic. Images were analyzed and cells were segmented using CellProfiler (v 4.2.4) analysis software. TO-PRO-3 staining intensity per object was measured and difference in signal between TO-PRO-3 stained versus unstained cells provided basis for live/dead cell filtering. After filtering live and dead cells, the proportion of live cells was used for viability analysis.

Glutamate titration

After 21 days of differentiation, CaMPARI2 iNeurons were treated with increasing concentrations of glutamate (0-500 µM) for 5 minutes. This was followed by CaMPARI photoconversion and dissociation (protocols as described above). The mean R/G ratio for each concentration, with 6 independent culture wells per measurement, was used to calculate a polynomial fit using Prism (v10.1.1). 30 µM was chosen for subsequent experiments and screens due to the potential dynamic range available to detect increases in activity (increase CaMPARI2 response) while still allowing for some dynamic range to sense decreases in activity (lower CaMPARI2 response).

CRISPR screens

Generation of sgRNA library

A custom CRISPRi library targeting genes associated neurological disease and activity (Neuron Activity library) was synthesized as follows: The disease-associated gene list were generated using DisGeNET[79] online database, using the neurodegenerative, neurodevelopment, and neuropsychiatric diseases highlighted in Figure 2c as search terms. This was supplemented using genes chosen by searching terms 'synapse', 'neurotransmitter', 'calcium', 'membrane potential', 'neuron activity', and 'neuron membrane' in GO, KEGG, Reactome and Wikipathways. This gene list was filtered for gene expressed in NGN2-iNeurons based of RNA sequencing data,[17] resulting in a final number of 1343 genes targeted in the library. The top 5 predicted sgRNAs[80] oligonucleotide sequences per gene plus 250 non-targeting control (NTC) sequences (for 7450 total library elements) were synthesized by Agilent Technologies (RRID:SCR_013575; Santa Clara, CA) on a 7.5K oligo array and cloned into the pLG15 sgRNA expression vector. Library complexity and the presence of each oligo was confirmed with Illumina next-generation sequencing.

Primary FACS based screen

The Neuron Activity library was packaged into lentivirus as previously described for the CRISPRi genome-wide sublibraries.[17] CRISPRi-NGN2-CaMPARI2 iPSCs were infected by the sgRNA library at MOIs between 0.3-0.5 (as measured by the BFP fluorescence in the sgRNA lentiviral vector) with >1000X coverage per library element. On the next passage, iPSCs expressing the sgRNA vector were selected using puromycin (see

above) as they were expanded for screening, limiting the total number of passages from lentiviral transduction to three to limit dropout of sgRNAs at the iPSC stage. iPSCs were scaled to a cell count corresponding to >10e^4 x coverage per library element for each FACS sorted population, and differentiated into neurons as described above. On day 0 of the differentiation, iNeurons were plated onto 15 cm poly-D-lysine-coated plates (Corning 354550) at a density of 138k/cm^2. iNeurons were maintained as described above until FACS sorting.

On day 21, iNeurons were treated with 30 µM glutamate for 5 minutes before photoconversion (described above). These were then dissociated with the above dissociation protocol, with the following modifications: incubation time in dissociation solution was increased to 20 minutes, papain was resuspended in 1:1 HBSS and Accutase, and dissociated neurons were resuspended in FACS wash buffer: 20 mL HBSS supplemented with 5 mM $MgCl_2$, 10 nM Y-27632, and 10 U/mL DNaseI. Resuspended iNeurons were maintained as a sheet, transferred to a 50 mL tube, vigorously triturated, then pelleted at 300xg for 10 minutes. After the supernatant was discarded, the pellet was resuspended in 1-2 mL of FACS wash buffer, using trituration to make a single-cell suspension. Resuspended iNeurons were sorted into high and low R/G ratio populations corresponding to the top 35% and bottom 35% of the R/G signal distribution (see gating strategy, Supplementary Information), followed by sample preparation for next-generation sequencing. This screen was conducted in duplicate.

Pooled secondary screens

The focused secondary screening library contained 1211 sgRNAs targeting 411 genes (3-5 sgRNAs per gene) that were hits in either of the replicate primary screens and 250 NTC sgRNAs (1622 total sgRNAs). sgRNAs were selected based on their phenotype in the primary screens. A pool of sgRNA-containing oligonucleotides were synthesized by Twist Biosciences (South San Francisco, CA, USA) and cloned into an optimized sgRNA lentivirus vector (pMK1334) as previously described.[18] CRISPRi-NGN2-CaMPARI2 iPSCs were transduced with lentivirus containing the secondary screening library, selected, and expanded as described for the primary screen above. A fraction of day 0 iNeurons were harvested and subjected to sample preparation for next-generation sequencing.

On day 21, iNeurons were treated with either 50 mM KCl or 30 µM glutamate, undergoing the same screening protocol as above.

Separately, CRISPRi-NGN2-CaMPARI2 iPSCs transduced with lentivirus were treated with 30 µM glutamate to match the same photoconversion conditions as day 21 iNeurons. These were then dissociated with Accutase (see Human iPSC Culture subsection) and sorted into high and low R/G ratio populations corresponding to the top 35% and bottom 35% of the R/G signal distribution, followed by sample preparation for next-generation sequencing.

Screen sample preparation

For each screen sample, genomic DNA was isolated using a Macherey-Nagel Nucleospin Blood kit (Macherey-Nagel; Cat. No. 740951.50) or Macherey-Nagel Nucleospin Blood L kit (Macherey-Nagel; Cat. No. 740954.20), depending on the number of cells recovered from FACS. sgRNA-encoding regions were amplified and sequenced on an Illumina HiSeq- 4000 as previously described.[17]

Validation of CRISPR screen hits

CaMPARI2 iNeurons expressing sgRNAs targeting hit genes were plated onto 96-well poly-D-lysine coated plates (Corning 354640) at 12,500 cells/well in BrainPhys neuronal media. The assay was internally controlled by plating an equal mixture of CaMPARI2 iNeurons expressing no sgRNA and knockdown iNeurons, to a final density of 25,000 cells/well (78,000 cells/cm^2).

qPCR

To quantify knockdown in CaMPARI2 cells, lysed cell pellets from human iPSCs or iNeurons were thawed on ice, and total RNA was extracted using Quick-RNA Miniprep Kit (Zymo; Cat. No. R1054). Complementary DNA was synthesized with the SensiFAST cDNA Synthesis Kit (Bioline; Cat. No. 65054). Samples were prepared for qPCR in technical triplicates in 10-µl reaction volumes using SensiFAST SYBR Lo-ROX 2X Master Mix (Bioline; Cat. No. BIO-94005), custom qPCR primers from Integrated DNA Technologies used at a final concentration of 0.2 µM and cDNA diluted at 1:3. qPCR was performed on an Applied Biosystems QuantStudio 6 Pro Real-Time PCR System using QuantStudio Real Time PCR software (v.1.3) with the following Fast 2-Step protocol: (1) 95 °C for 20 s; (2) 95 °C for 5 s (denaturation); (3) 60 °C for 20 s (annealing/extension); (4) repeat steps 2 and 3 for a total of 40 cycles; (5) 95 °C for 1 s; (6) ramp 1.92 °C s^{-1} from 60 °C to 95 °C to establish melting curve. Expression fold changes were calculated using the ΔΔCt method, and normalized to housekeeping gene *GAPDH*. Primer sequences are provided in Supplementary Table 5.

Electrophysiology

Patch clamp electrophysiology measurements were made using a Multiclamp 700B amplifier, with pClamp10 acquisition software (Molecular Devices). Recordings were filtered at 2 kHz for voltage clamp or at 10 kHz for current clamp. Digitization was performed at a frequency of 10 kHz, with a Digidata 1440 analog-to-digital converter (Molecular Devices). For current clamp recordings the intracellular solution was composed of (in mM): 130 K-gluconate, 5 NaCl, 10 HEPES, 0.2 EGTA, 2 $MgCl_2$, 4 Na-ATP, 0.5 Mg-GTP, with a pH of 7.3. For voltage clamp recordings, the intracellular solution was composed of (in mM): 130 $CsMeSO_3$, 4 NaCl, 10 HEPES, 0.2 EGTA, 5 QX-314 Br, 4 Na-ATP, 0.5 Mg-GTP, with a pH of 7.3.

The recording chamber was continuously infused with oxygenated ACSF, which contained (in mM): 127 NaCl, 2.5 KCl, 1.25 $NaHPO_4$, 25 Na_2CO_3, 25 glucose, 2.5 CaCl2, 1.3 MgCl2. Recording electrodes had an open-tip resistance between 4-8 MΩ. These recordings were performed 2-3 weeks after the RNP-CRISPR knockout procedure. Data for each gene was collated from two batches of iNeuron cultures.

Specific electrophysiology protocols for individual validation of hit genes:

For the *KCNT2* knockout and NTC iNeurons, the current-spike output relationship was measured as follows: Cells were current-clamped at -70 mV. A sequence of 20 x 1 second long current steps were injected, starting from -20 pA and increased by 10 pA for each step.

For *CACNG2* knockout and NTC iNeurons, spontaneous excitatory postsynaptic currents (sEPSC) were recorded for 1 minute while the cells were voltage clamped at -70 mV. In cases where no events were observed during the initial minute, an additional minute of recording was performed. To enhance the detection of synaptic events, the synaptic vesicle release probability was increased in these experiments by elevating KCl to 5 mM and CaCl2 to 4 mM with zero MgCl2 in ACSF.

For *PICALM* knockout and NTC iNeurons, cells were voltage clamped at -70 mV and +40 mV for one minute to measure sEPSCs. If no events were observed within the initial minute, the recordings were performed for an additional minute. AMPA receptor-mediated sEPSCs were isolated by adding either 50 µM D-AP5 or 100 µM DL-AP5 (Cat. No. 0106Tocris) to the recording solution. Addition of 100 µM cyclothiazide (Cat. No.0713, Tocris or Cat. No. ALX-550-338-M050 Enzo) was used to reduce AMPA receptor desensitization and facilitate the detection of synaptic events. 100 µM spermine (Cat. No. S3256 Sigma-Aldrich) was included in the intracellular solution to block calcium-permeable AMPA receptors at +40 mV, aiding in the quantification of the rectification index (mean sEPSC current amplitude at +40 mV / mean sEPSC current amplitude at -70 mV).

All recordings were analyzed using Easy Electrophysiology software (v2.6, Cambridge, UK). The minimum current step that initiated action potential firing was defined as the rheobase. The maximum firing rate was calculated at the current step that initiated the highest number of action potentials, with no failure being observed. The action potential half-width was computed from the first action potential at the rheobase. Recordings were included for analysis if a minimum of 5 sEPSC events were detected during the recording time frame (0.08Hz). Charge transfer for each recording was computed as the frequency * 60 seconds * the charge transfer for the average sEPSCs. Statistical analyses were performed using GraphPad Prism (v10.1.1; GraphPad Software; Boston,

MA, USA) including the Mann-Whitney test or an ANOVA, followed by the Kruskal-Wallis test for multiple comparisons.

Data Analysis

CRISPR screen analysis

Primary screens were analyzed using sgcount and crispr_screen, two publicly available Rust packages based on MAGeCK[81] and our previously published MAGeCK-iNC bioinformatics pipeline.[17] The packages sgcount and crispr_screen are available on the Kampmann Lab website (https://kampmannlab.ucsf.edu/sgcount, https://kampmannlab.ucsf.edu/crisprscreen) and on Github (https://github.com/noamteyssier/sgcount, https://github.com/noamteyssier/crispr_screen).

Briefly, raw sequencing reads from next-generation sequencing are analyzed for the variable region (sgRNA protospacer sequence). Sequences in each sample are cropped to remove adapter regions and non-variable sequences to leave protospacer sequences remaining. These are then mapped to a sgRNA reference library to generate a count matrix for each screen sample. The quality of each screen was assessed by plotting the $\log_{10}$(counts) per sgRNA on a rank order plot using ggplot2.

Log_2 fold change and significance P values were calculated for target genes over 'negative-control-quasi-genes', as well as an FDR given the 'negative-control-quasi-genes' that were generated by random sampling with replacement of five NTC sgRNAs from all NTC sgRNAs (iNC method). A 'Gene Score' was defined as the product of $\log_2$ fold change and −log10(P value). Hit genes were determined based on the p value cut-off corresponding to an empirical false discovery rate of 10%. Volcano plots of $\log_2$ fold change vs -$\log_{10}$(p value) and scatter plots of Gene Scores were generated using ggplot2.

Over-representation analysis with WebGestalt

Hit genes from the primary screen were separated into hits decreasing and increasing activity. These lists were input into WebGestaltR[37] (version 0.4.6) and enriched with the ORA method. The screening library was used as the reference gene list. Significant terms were thresholded at a FDR of 0.1, using Benjamini Hochberg.

Image analysis with CellProfiler

Pipelines and example images are compiled in supplementary material, and all analyzes were performed using CellProfiler v.4.1.3. Cell toxicity by TO-PRO-3 co-localization: Nuclei were segmented as primary objects from Hoechst and TO-PRO-3

images. TO-PRO-3 objects that overlapped with Hoechst objects were counted as dead cells, while Hoechst objects negative for TO-PRO-3 were counted as live cells.

Software

GraphPad Prism v10.1.1; GraphPad Software; Boston, MA, USA

FlowJo analysis software v10.10.0; BD Life Sciences; Ashland, OR, USA

RStudio v2023.06.1+524 RStudio, PBC, Boston, MA, USA

Easy Electrophysiology software; v2.6; Cambridge, UK

R packages used for presentation of data:

tidyverse, ggrepel, ggpubr, reshape2, dplyr, ggplot2, grid, WebGestaltR, extrafont, viridis, RColorBrewer, ggthemes, remotes, circlize, corrplot, Hmisc.

Statistics and reproducibility

No statistical methods were used to pre-determine sample sizes but our sample sizes are similar to those reported in previous publications.[17–19] No randomization of samples was used since treatment group of cells were generally derived from the same population of cells. Data collection and analysis were not performed blind to the conditions of the experiments. No data points were excluded from analysis. Data distribution was assumed to be normal but this was not formally tested.

Reporting summary

Further information on research design is available in the Nature Research Reporting Summary linked to this article.

Data availability

All screen datasets will be shared on the CRISPRbrain data commons (http://crisprbrain.org/) and will be shared upon request (associated with Figs. 2 and 4 and Extended Data Fig. 2). There are no restrictions on data availability.

Code availability

The sgcount and crispr_screen bioinformatics pipelines for analysis of pooled screens are available on the Kampmann Lab website (https://kampmannlab.ucsf.edu/sgcount, https://kampmannlab.ucsf.edu/crisprscreen) and on Github (https://github.com/noamteyssier/sgcount, https://github.com/noamteyssier/crispr_screen). The CellProfiler pipelines will be made available on request to the corresponding authors (M.K.) and will also be submitted to the CellProfiler depository of published pipelines (https://cellprofiler.org/examples/published_pipelines.html) upon publication.

Availability of biological materials

All materials can be requested from the corresponding author (M.K.) and will be made available without restrictions via a material transfer agreement.

Acknowledgements

We would like to thank Nick Page (UCSF) for contributions to preliminary experiments, the Weill Imaging Core and the Center for Advanced Light Microscopy, including Caroline Mrejen, So Yeon Kim, and Kari Herrington, for their technical support and microscopy instrumentation, the Laboratory for Cell Analysis and Sarah Elmes for use of FACS instruments.

We would like to thank Scott Martin, Ana Jovicic, and the Genentech Research and Early Development team (gRED) for their helpful discussions.

The authors would also like to thank Olivia Teter, Avi Samelson, and Kunal Shroff for helpful comments and suggestions during the writing of this manuscript.

This research was funded by an award by the Alliance for Therapies in Neuroscience (ATN, Genentech and the University of California San Francisco) to M.K., an Alzheimer's Association Research Fellowship to S.C.B. (23AARF-1027616), a California Institute for Regenerative Medicine (CIRM) grant to J.Y.C. (EDUC2-12730), a Rainwater Charitable Foundation Tau Consortium Investigator award, a Ben Barres Early Career Acceleration award by the Chan Zuckerberg Initiative , and NIH/NINDS grant U54 NS123746 to M.K.

Author contributions

Conceptualization of the CaMPARI2 based screen strategy was done by S.C.B, R.T, and M.K. CRISPRi screens and individual validation of screen hits were performed by S.C.B, V.G., and J.Y.C. sgRNA constructs for KD validation experiments were synthesized by S.C.B, V.G., J.Y.C, and L.Y. CRISPR-RNP KOs in iPSC-neurons was performed by X. H. and C.E. Electrophysiology was performed by M.T. with input from J.H. CRISPR screen analysis was performed by S.C.B. with an analysis pipeline

developed by N.T.. S.C.B, V.G., and M.T. created the figures, with input from all authors. S.C.B and M.K wrote the manuscript with input from all authors. All authors reviewed and approved the final manuscript.

Competing interests

M.K. is a co-scientific founder of Montara Therapeutics and serves on the Scientific Advisory Boards of Engine Biosciences, Casma Therapeutics, Cajal Neuroscience, Alector, and Montara Therapeutics, and is an advisor to Modulo Bio and Recursion Therapeutics. M.K. is an inventor on US Patent 11,254,933 related to CRISPRi and CRISPRa screening, and on a US Patent application on *in vivo* screening methods. M.T., X.H., C.E., and J.H. are employees of Genentech.

References

1. Fang, R. *et al.* Conservation and divergence of cortical cell organization in human and mouse revealed by MERFISH. *Science* **377**, 56–62 (2022).
2. Jorstad, N. L. *et al.* Transcriptomic cytoarchitecture reveals principles of human neocortex organization. *Science* **382**, eadf6812 (2023).
3. Yao, Z. *et al.* A high-resolution transcriptomic and spatial atlas of cell types in the whole mouse brain. *Nature* **624**, 317–332 (2023).
4. Jin, K. *et al.* Cell-type specific molecular signatures of aging revealed in a brain-wide transcriptomic cell-type atlas. 2023.07.26.550355 Preprint at https://doi.org/10.1101/2023.07.26.550355 (2023).
5. Camunas-Soler, J. *et al.* Patch-Seq Links Single-Cell Transcriptomes to Human Islet Dysfunction in Diabetes. *Cell Metabolism* **31**, 1017-1031.e4 (2020).
6. International League Against Epilepsy Consortium on Complex Epilepsies. GWAS meta-analysis of over 29,000 people with epilepsy identifies 26 risk loci and subtype-specific genetic architecture. *Nat Genet* **55**, 1471–1482 (2023).
7. Guerrini, R., Balestrini, S., Wirrell, E. C. & Walker, M. C. Monogenic Epilepsies. *Neurology* **97**, 817–831 (2021).
8. Kunkle, B. W. *et al.* Genetic meta-analysis of diagnosed Alzheimer's disease identifies new risk loci and implicates Aβ, tau, immunity and lipid processing. *Nat Genet* **51**, 414–430 (2019).
9. Satterstrom, F. K. *et al.* Large-Scale Exome Sequencing Study Implicates Both Developmental and Functional Changes in the Neurobiology of Autism. *Cell* **180**, 568-584.e23 (2020).
10. Zhang, Y. & Looger, L. L. Fast and sensitive GCaMP calcium indicators for neuronal imaging. *J Physiol* (2023) doi:10.1113/JP283832.
11. Knöpfel, T. & Song, C. Optical voltage imaging in neurons: moving from technology development to practical tool. *Nat Rev Neurosci* **20**, 719–727 (2019).
12. Liu, P. & Miller, E. W. Electrophysiology, Unplugged: Imaging Membrane Potential with Fluorescent Indicators. *Acc Chem Res* **53**, 11–19 (2020).
13. Deisseroth, K. Optogenetics. *Nat Methods* **8**, 26–29 (2011).
14. Kim, C. K., Adhikari, A. & Deisseroth, K. Integration of optogenetics with complementary methodologies in systems neuroscience. *Nat Rev Neurosci* **18**, 222–235 (2017).
15. Boivin, B. *et al.* A multiparametric activity profiling platform for neuron disease phenotyping and drug screening. *Mol Biol Cell* **33**, ar54 (2022).
16. Gilbert, L. A. *et al.* Genome-Scale CRISPR-Mediated Control of Gene Repression and Activation. *Cell* **159**, 647–661 (2014).
17. Tian, R. *et al.* CRISPR Interference-Based Platform for Multimodal Genetic Screens in Human iPSC-Derived Neurons. *Neuron* **104**, 239-255.e12 (2019).
18. Tian, R. *et al.* Genome-wide CRISPRi/a screens in human neurons link lysosomal failure to ferroptosis. *Nat Neurosci* **24**, 1020–1034 (2021).
19. Dräger, N. M. *et al.* A CRISPRi/a platform in human iPSC-derived microglia uncovers regulators of disease states. *Nat Neurosci* **25**, 1149–1162 (2022).
20. Leng, K. *et al.* CRISPRi screens in human iPSC-derived astrocytes elucidate regulators of distinct inflammatory reactive states. *Nat Neurosci* (2022) doi:10.1038/s41593-022-01180-9.

21. Li, E. *et al.* CRISPRi-based screens in iAssembloids to elucidate neuron-glia interactions. 2023.04.26.538498 Preprint at https://doi.org/10.1101/2023.04.26.538498 (2023).
22. Samelson, A. J. *et al.* CRISPR screens in iPSC-derived neurons reveal principles of tau proteostasis. 2023.06.16.545386 Preprint at https://doi.org/10.1101/2023.06.16.545386 (2023).
23. Ebner, C. *et al.* Optically Induced Calcium-Dependent Gene Activation and Labeling of Active Neurons Using CaMPARI and Cal-Light. *Front Synaptic Neurosci* **11**, 16 (2019).
24. Trojanowski, N. F., Bottorff, J. & Turrigiano, G. G. Activity labeling in vivo using CaMPARI2 reveals intrinsic and synaptic differences between neurons with high and low firing rate set points. *Neuron* **109**, 663-676.e5 (2021).
25. Zolnik, T. A. *et al.* All-optical functional synaptic connectivity mapping in acute brain slices using the calcium integrator CaMPARI: CaMPARI for all-optical functional connectivity mapping *ex vivo*. *J Physiol* **595**, 1465–1477 (2017).
26. Moeyaert, B. *et al.* Improved methods for marking active neuron populations. *Nat Commun* **9**, 4440 (2018).
27. Perdigão, C. *et al.* Intracellular Trafficking Mechanisms of Synaptic Dysfunction in Alzheimer's Disease. *Front Cell Neurosci* **14**, 72 (2020).
28. Zoghbi, H. Y. & Bear, M. F. Synaptic Dysfunction in Neurodevelopmental Disorders Associated with Autism and Intellectual Disabilities. *Cold Spring Harbor Perspectives in Biology* **4**, a009886–a009886 (2012).
29. Hoover, B. R. *et al.* Tau mislocalization to dendritic spines mediates synaptic dysfunction independently of neurodegeneration. *Neuron* **68**, 1067–1081 (2010).
30. Li, K. *et al.* Synaptic Dysfunction in Alzheimer's Disease: Aβ, Tau, and Epigenetic Alterations. *Mol Neurobiol* **55**, 3021–3032 (2018).
31. Keller, R., Basta, R., Salerno, L. & Elia, M. Autism, epilepsy, and synaptopathies: a not rare association. *Neurol Sci* **38**, 1353–1361 (2017).
32. Vossel, K. A. *et al.* Seizures and epileptiform activity in the early stages of Alzheimer disease. *JAMA Neurol* **70**, 1158–1166 (2013).
33. Vossel, K. A. *et al.* Incidence and impact of subclinical epileptiform activity in Alzheimer's disease. *Annals of Neurology* **80**, 858–870 (2016).
34. Beagle, A. J. *et al.* Relative Incidence of Seizures and Myoclonus in Alzheimer's Disease, Dementia with Lewy Bodies, and Frontotemporal Dementia. *J Alzheimers Dis* **60**, 211–223 (2017).
35. Palop, J. J. & Mucke, L. Network abnormalities and interneuron dysfunction in Alzheimer disease. *Nat Rev Neurosci* **17**, 777–792 (2016).
36. Zimmern, V., Minassian, B. & Korff, C. A Review of Targeted Therapies for Monogenic Epilepsy Syndromes. *Front Neurol* **13**, 829116 (2022).
37. Wang, J., Vasaikar, S., Shi, Z., Greer, M. & Zhang, B. WebGestalt 2017: a more comprehensive, powerful, flexible and interactive gene set enrichment analysis toolkit. *Nucleic Acids Research* **45**, W130–W137 (2017).
38. Krukowski, K. *et al.* Small molecule cognitive enhancer reverses age-related memory decline in mice. *eLife* **9**, e62048 (2020).

39. Costa-Mattioli, M. *et al.* eIF2alpha phosphorylation bidirectionally regulates the switch from short- to long-term synaptic plasticity and memory. *Cell* **129**, 195–206 (2007).
40. Sharma, V. *et al.* eIF2α controls memory consolidation via excitatory and somatostatin neurons. *Nature* **586**, 412–416 (2020).
41. Larsson, M., Agalave, N., Watanabe, M. & Svensson, C. I. Distribution of transmembrane AMPA receptor regulatory protein (TARP) isoforms in the rat spinal cord. *Neuroscience* **248**, 180–193 (2013).
42. Yamasaki, M. *et al.* TARP γ-2 and γ-8 Differentially Control AMPAR Density Across Schaffer Collateral/Commissural Synapses in the Hippocampal CA1 Area. *J Neurosci* **36**, 4296–4312 (2016).
43. Bats, C., Groc, L. & Choquet, D. The Interaction between Stargazin and PSD-95 Regulates AMPA Receptor Surface Trafficking. *Neuron* **53**, 719–734 (2007).
44. Chen, L. *et al.* Stargazin regulates synaptic targeting of AMPA receptors by two distinct mechanisms. *Nature* **408**, 936–943 (2000).
45. Adotevi, N. K. & Leitch, B. Alterations in AMPA receptor subunit expression in cortical inhibitory interneurons in the epileptic stargazer mutant mouse. *Neuroscience* **339**, 124–138 (2016).
46. Jackson, A. C. & Nicoll, R. A. The Expanding Social Network of Ionotropic Glutamate Receptors: TARPs and Other Transmembrane Auxiliary Subunits. *Neuron* **70**, 178–199 (2011).
47. Liu, R. *et al.* Increased Expression of KNa1.2 Channel by MAPK Pathway Regulates Neuronal Activity Following Traumatic Brain Injury. *Neurochem Res* (2023) doi:10.1007/s11064-023-04044-1.
48. Oguro, K. *et al.* Knockdown of AMPA Receptor GluR2 Expression Causes Delayed Neurodegeneration and Increases Damage by Sublethal Ischemia in Hippocampal CA1 and CA3 Neurons. *J Neurosci* **19**, 9218–9227 (1999).
49. Friedman, L. K. Selective reduction of GluR2 protein in adult hippocampal CA3 neurons following status epilepticus but prior to cell loss. *Hippocampus* **8**, 511–525 (1998).
50. Smeets, C. J. L. M., Ma, K. Y., Fisher, S. E. & Verbeek, D. S. Cerebellar developmental deficits underlie neurodegenerative disorder spinocerebellar ataxia type 23. *Brain Pathol* **31**, 239–252 (2020).
51. Parsons, R. Discovery of the PTEN Tumor Suppressor and Its Connection to the PI3K and AKT Oncogenes. *Cold Spring Harb Perspect Med* **10**, a036129 (2020).
52. Wang, L., Lu, G. & Shen, H.-M. The Long and the Short of PTEN in the Regulation of Mitophagy. *Frontiers in Cell and Developmental Biology* **8**, (2020).
53. Williams, M. R., DeSpenza, T., Li, M., Gulledge, A. T. & Luikart, B. W. Hyperactivity of Newborn Pten Knock-out Neurons Results from Increased Excitatory Synaptic Drive. *J Neurosci* **35**, 943–959 (2015).
54. Azarnia Tehran, D. *et al.* Selective endocytosis of Ca2+-permeable AMPARs by the Alzheimer's disease risk factor CALM bidirectionally controls synaptic plasticity. *Science Advances* **8**, eabl5032 (2022).
55. García-Cabrero, A. M. *et al.* Hyperexcitability and epileptic seizures in a model of frontotemporal dementia. *Neurobiol Dis* **58**, 200–208 (2013).

56. Wainger, B. J. *et al.* Intrinsic Membrane Hyperexcitability of Amyotrophic Lateral Sclerosis Patient-Derived Motor Neurons. *Cell Reports* **7**, 1–11 (2014).
57. Gomez-Murcia, V. *et al.* Hyperexcitability and seizures in the THY-Tau22 mouse model of tauopathy. *Neurobiol Aging* **94**, 265–270 (2020).
58. Telias, M. Molecular Mechanisms of Synaptic Dysregulation in Fragile X Syndrome and Autism Spectrum Disorders. *Front Mol Neurosci* **12**, 51 (2019).
59. Trimmer, J. S. Subcellular localization of K+ channels in mammalian brain neurons: remarkable precision in the midst of extraordinary complexity. *Neuron* **85**, 238–256 (2015).
60. Yang, B., Desai, R. & Kaczmarek, L. K. Slack and Slick KNa Channels Regulate the Accuracy of Timing of Auditory Neurons. *J Neurosci* **27**, 2617–2627 (2007).
61. Kim, G. E. & Kaczmarek, L. K. Emerging role of the KCNT1 Slack channel in intellectual disability. *Front Cell Neurosci* **8**, 209 (2014).
62. Møller, R. S. *et al.* Mutations in KCNT1 cause a spectrum of focal epilepsies. *Epilepsia* **56**, e114–e120 (2015).
63. Gong, P., Jiao, X., Yu, D. & Yang, Z. Case Report: Causative De novo Variants of KCNT2 for Developmental and Epileptic Encephalopathy. *Front Genet* **12**, 649556 (2021).
64. Ambrosino, P. *et al.* De novo gain-of-function variants in KCNT2 as a novel cause of developmental and epileptic encephalopathy. *Ann Neurol* **83**, 1198–1204 (2018).
65. Dreyling, M. H. *et al.* The t(10;11)(p13;q14) in the U937 cell line results in the fusion of the AF10 gene and CALM, encoding a new member of the AP-3 clathrin assembly protein family. *Proc Natl Acad Sci U S A* **93**, 4804–4809 (1996).
66. Tebar, F., Bohlander, S. K. & Sorkin, A. Clathrin Assembly Lymphoid Myeloid Leukemia (CALM) Protein: Localization in Endocytic-coated Pits, Interactions with Clathrin, and the Impact of Overexpression on Clathrin-mediated Traffic. *Mol Biol Cell* **10**, 2687–2702 (1999).
67. Harold, D. *et al.* Genome-wide association study identifies variants at CLU and PICALM associated with Alzheimer's disease. *Nat Genet* **41**, 1088–1093 (2009).
68. Bellenguez, C. *et al.* New insights into the genetic etiology of Alzheimer's disease and related dementias. *Nat Genet* **54**, 412–436 (2022).
69. Jun, G. *et al.* Meta-Analysis confirms CR1, CLU, and PICALM as Alzheimer's disease risk loci and reveals interactions with APOE genotypes. *Arch Neurol* **67**, 1473–1484 (2010).
70. Lambert, J.-C. *et al.* Evidence of the association of BIN1 and PICALM with the AD risk in contrasting European populations. *Neurobiology of Aging* **32**, 756.e11-756.e15 (2011).
71. Moreau, K. *et al.* PICALM modulates autophagy activity and tau accumulation. *Nat Commun* **5**, 4998 (2014).
72. Sanchez, M. I., Nguyen, Q.-A., Wang, W., Soltesz, I. & Ting, A. Y. Transcriptional readout of neuronal activity via an engineered Ca2+-activated protease. *PNAS* **117**, 33186–33196 (2020).
73. Kim, C. K. *et al.* A Molecular Calcium Integrator Reveals a Striatal Cell Type Driving Aversion. *Cell* **183**, 2003-2019.e16 (2020).
74. Bardy, C. *et al.* Neuronal medium that supports basic synaptic functions and activity of human neurons in vitro. *Proc Natl Acad Sci USA* **112**, E2725–E2734 (2015).

75. Satir, T. M. *et al.* Accelerated neuronal and synaptic maturation by BrainPhys medium increases Aβ secretion and alters Aβ peptide ratios from iPSC-derived cortical neurons. *Sci Rep* **10**, 601 (2020).
76. Shih, P.-Y. *et al.* Development of a fully human assay combining NGN2-inducible neurons co-cultured with iPSC-derived astrocytes amenable for electrophysiological studies. *Stem Cell Research* **54**, 102386 (2021).
77. Meijer, M. *et al.* A Single-Cell Model for Synaptic Transmission and Plasticity in Human iPSC-Derived Neurons. *Cell Reports* **27**, 2199-2211.e6 (2019).
78. Nehme, R. *et al.* Combining NGN2 Programming with Developmental Patterning Generates Human Excitatory Neurons with NMDAR-Mediated Synaptic Transmission. *Cell Reports* **23**, 2509–2523 (2018).
79. Piñero, J. *et al.* The DisGeNET knowledge platform for disease genomics: 2019 update. *Nucleic Acids Research* **48**, D845–D855 (2020).
80. Horlbeck, M. A. *et al.* Compact and highly active next-generation libraries for CRISPR-mediated gene repression and activation. *eLife* **5**, e19760 (2016).
81. Li, W. *et al.* MAGeCK enables robust identification of essential genes from genome-scale CRISPR/Cas9 knockout screens. *Genome Biol* **15**, 554 (2014).

Figures

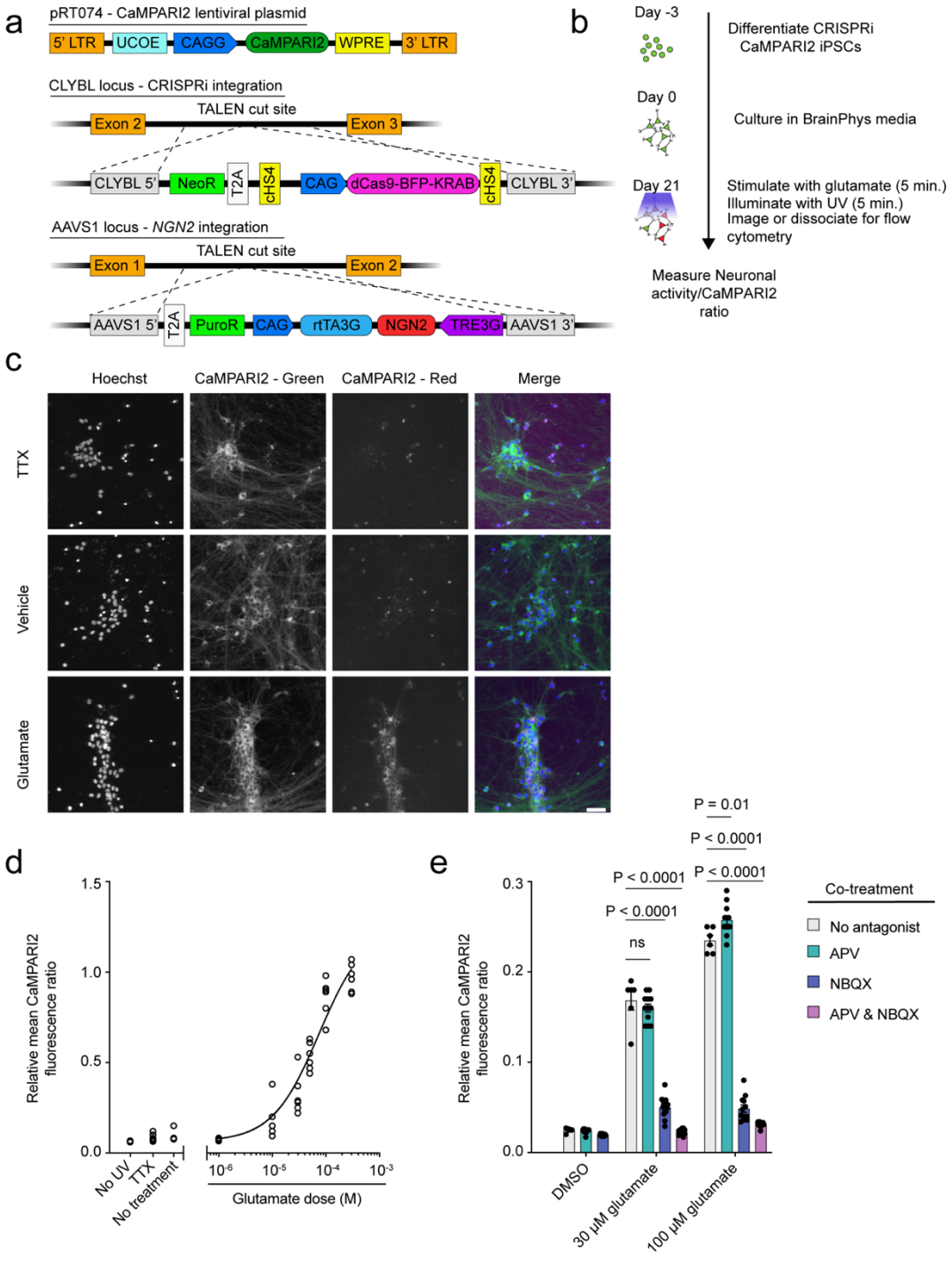

Figure 1. CaMPARI2 captures glutamate receptor activation in iPSC-derived glutamatergic neurons.

(a) Strategy for generating CRISPRi-NGN2-CaMPARI2 iPSC line: NGN2 and dCAS9-KRAB was stably integrated into the AAVS1 and CLYBL loci,

respectively, as described previously.[17] CAG promoter-driven CaMPARI2 was randomly inserted into the genome via lentiviral integration. UCOE: Ubiquitous Chromatin Opening Element, WPRE: Woodchuck Hepatitis Virus Posttranscriptional Regulatory Element.

(b) Experimental workflow of CaMPARI2 photoconversion assay in glutamatergic NGN2 neurons.

(c) Representative fluorescence micrographs of iPSC-neurons expressing CaMPARI2 following incubation with 1.5 µM tetrodotoxin (TTX), vehicle (0.1% DMSO), or 30 µM glutamate for 5 minutes and illumination with 405 nm light. Nuclei were stained with Hoechst 33342. Unconverted CaMPARI2 persists in the soma and neurites, and converted CaMPARI2 is only observed with high signal after incubation with 30 µM glutamate. Merged micrographs show colocalization of nuclei (blue), CaMPARI2 (green), and converted CaMPARI2 (magenta). Scale bar is 20 µm.

(d) CaMPARI2 neurons respond to glutamate in a dose-dependent manner. N = 6 independent culture wells per measurement. “No UV”, TTX (1.5 µM), and “no treatment” conditions did not contain glutamate.

(e) Co-incubation of glutamate with AMPA receptor (10 mM NBQX), but not NMDA receptor (50 mM APV), antagonists attenuate CaMPARI2 photoconversion, suggesting that AMPA receptor activation is the primary mechanism of calcium influx. N = 6 independent culture wells per measurement. Unpaired t-test, * = $P < 0.0001$. Error bars are SEM.3

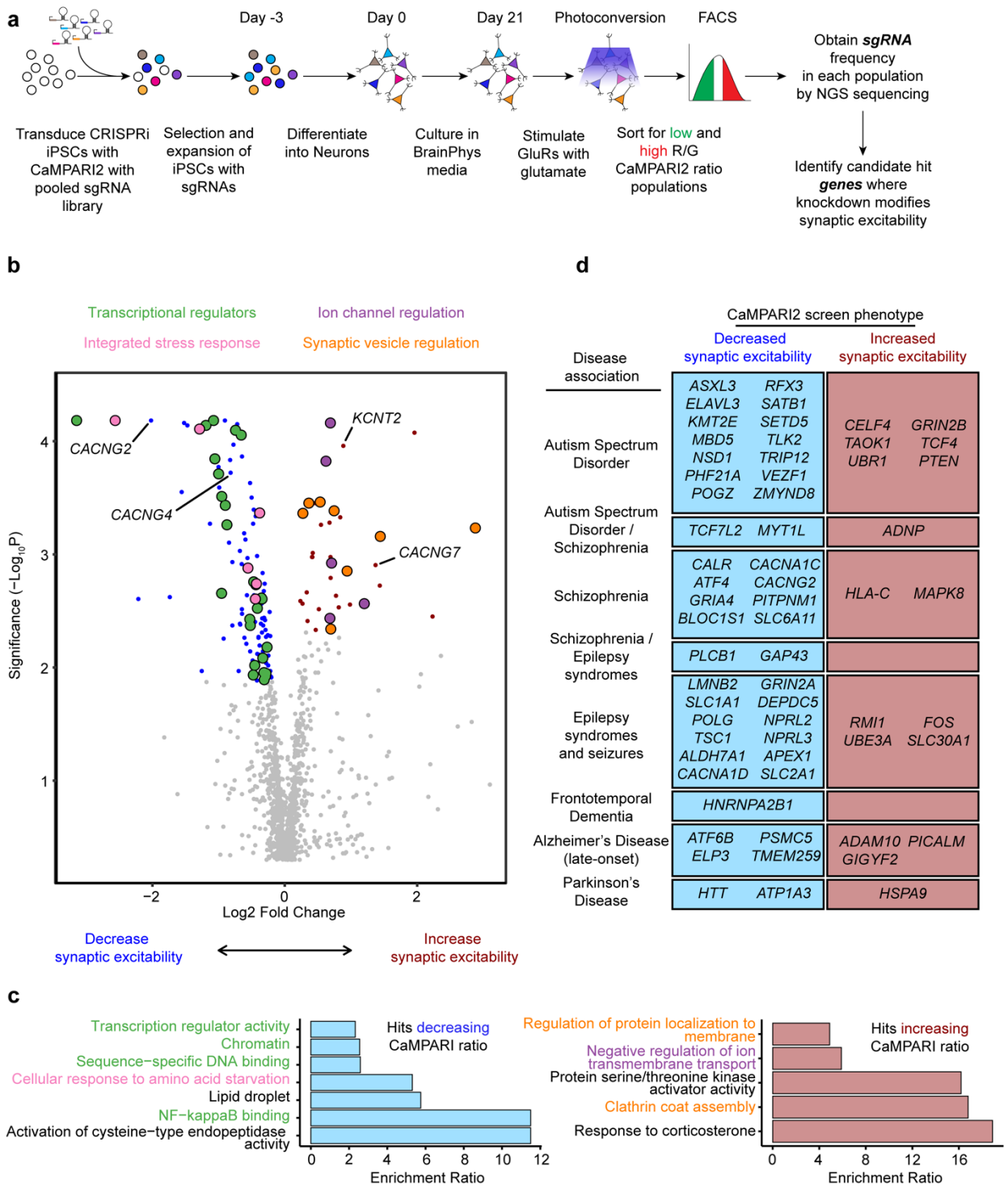

Figure 2. CRISPR interference (CRISPRi) screening with CaMPARI2 reveals genetic modifiers of neuronal excitability in iPSC derived neurons.

(a) Screening strategy using CaMPARI2 as readout for neuronal excitability. CRISPRi iPSC expressing CaMPARI2 were transduced with a lentiviral sgRNA

library focused on genes annotated for neuronal activity, neurodegenerative disease, or neurodevelopmental disorders (7449 sgRNA constructs targeting 1343 genes). Exposure to puromycin selects for iPSCs successfully transduced with sgRNA construct. iPSCs were then differentiated into neurons via overexpression of NGN2 and cultured for 21 days. Neurons were then incubated with 30 μM glutamate for five minutes, illuminated with UV light for five minutes, and then separated by FACS into high and low red/green fluorescence ratio populations. Frequency of neurons expressing sgRNAs were determined by next-generation sequencing for high and low red/green ratio neuronal populations and hit genes were identified.

(b) Volcano plot summarizing the effect of knockdowns on CaMPARI phenotypes and the determine statistical significance for targeted genes (Mann-Whitney U test). Dashed lines indicate a false-discovery rate (FDR) cutoff of 0.05, based on the phenotype score for genes calculated from 5 targeting sgRNAs. Red and blue points indicate hit genes where knockdown increases and decreases CaMPARI2 red/green fluorescence ratio, respectively, in response to glutamate stimulation. Grey points indicate non-hits. Large colored dots indicate hit genes that were found in the enriched GO terms in (d).

(c) Disease-associated genes that had an effect on synaptic excitability in the CaMPARI2 screen.

(d) Over-representation analysis (ORA) using Webgestalt indicates gene ontology (GO) annotation terms that describe genes enriched in the low (blue) and high (red) CaMPARI2 ratio from the screening library.

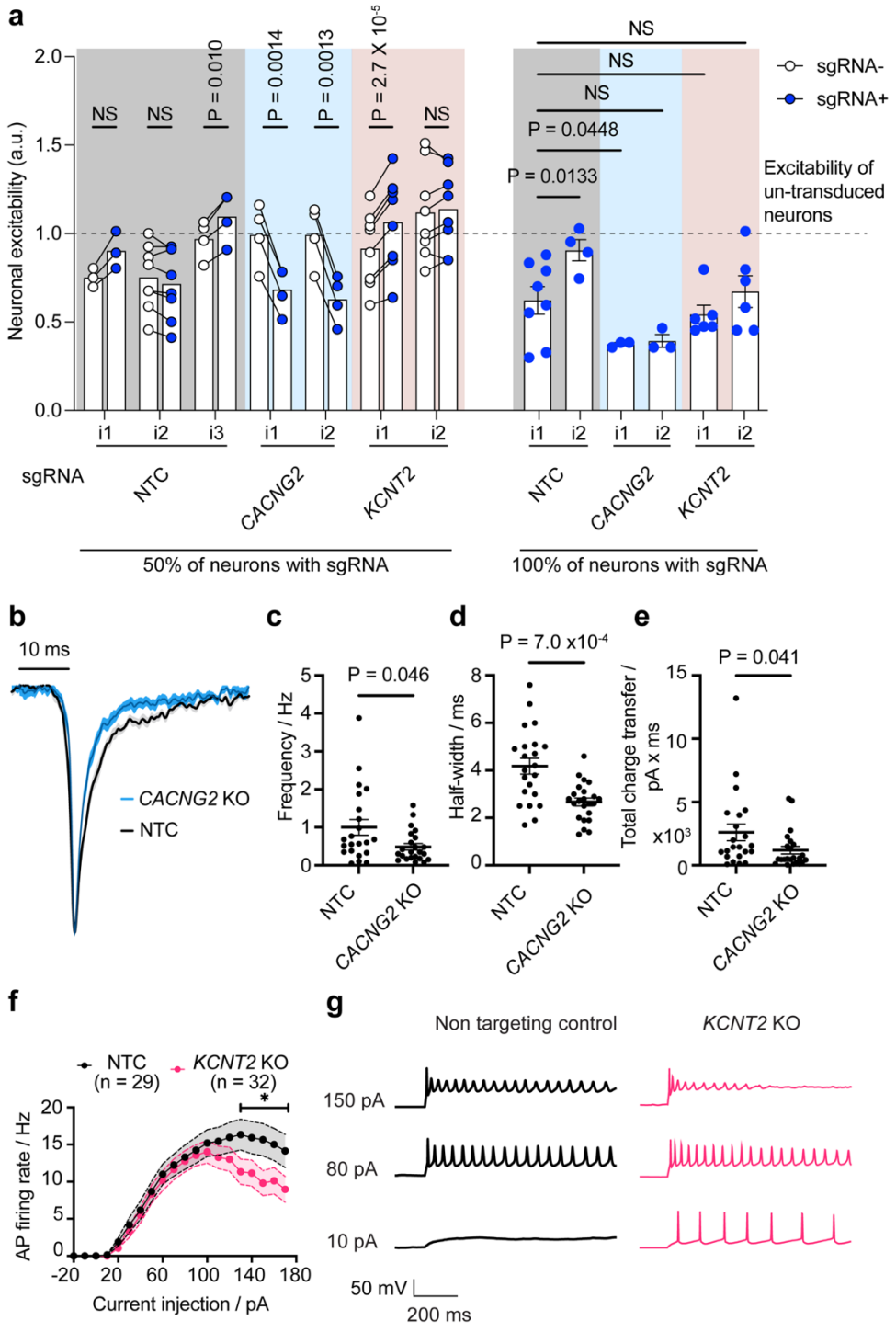

Figure 3. *CACNG2* and *KCNT2* modify excitability in human neurons.

(a) CaMPARI2 neurons expressing sgRNAs targeting *CACNG2* have reduced neuronal excitability in response to glutamate stimulation. This effect is observed intra-well, where *CACNG2* sgRNA-containing neurons have a lower CaMPARI2 ratio than those that do not receive the sgRNA, and inter-well, in cultures in which 100% of the neurons are expressing the sgRNA. One of the sgRNAs

targeting *KCNT2* shows an increase in neuronal excitability when comparing intra-well effects, which matches the screening phenotype. In cultures where 100% of the neurons are expressing one of the sgRNAs targeting *KCNT2*, there is an unexpected decrease in the observed neuronal excitability. CaMPARI2 ratios are normalized to neuron samples that do not receive a sgRNA and are run on the flow cytometer on the same day. 50% knockdown cultures : N = 3-8 independent culture wells per experiment. Each individual experiment was normalized to the excitability (CaMPARI2 response) of wells where neurons did not receive a sgRNA. For intra-well comparisons, a paired ratio t-test between sgRNA- and sgRNA+ populations were performed for each sgRNA. The calculated P values are corrected for multiple hypothesis (Holm-Šídák method). For inter-well comparisons, P values were calculated by ANOVA, using NTC_i1 as reference. $P > 0.05$ = not significant (NS).

(b) The spontaneous excitatory postsynaptic currents (sEPSCs) in *CACNG2* KO iNeurons demonstrate accelerated kinetics and a decrease in overall charge transfer. Averaged and normalized sEPSCs from all the recorded instances of NTCs (N = 22, in black) and *CACNG2* KOs (N = 23, in blue), with the shaded area indicating standard errors.

(c) *CACNG2* KOs exhibit reduced sEPSC frequency,

(d) half-width, and

(e) total charge transfer (Mann-Whitney test). NTCs (N = 22) and *CACNG2* KOs (N = 23). Error bars denote standard error.

(f) *KCNT2* KO neurons exhibit premature action potential failure. Current-spike output relationship presenting a diminished action potential firing rate in *KCNT2* KOs (N = 32) at high current injection amplitudes, as juxtaposed against non-targeting controls (N = 29). The differences were statistically significant for current injection steps greater than 120 pA (asterisk donates p values as follows: 130 pA: $p = 0.01$, 140 pA : $p = 0.02$, 150 pA: $p < 0.01$, 160 pA: $p = 0.02$, 170 pA: $p = 0.01$; two-way ANOVA with multiple comparisons).

(g) Sample recordings from both NTCs and *KCNT2* KOs illustrating voltage responses of neurons to varying degrees of current injection.

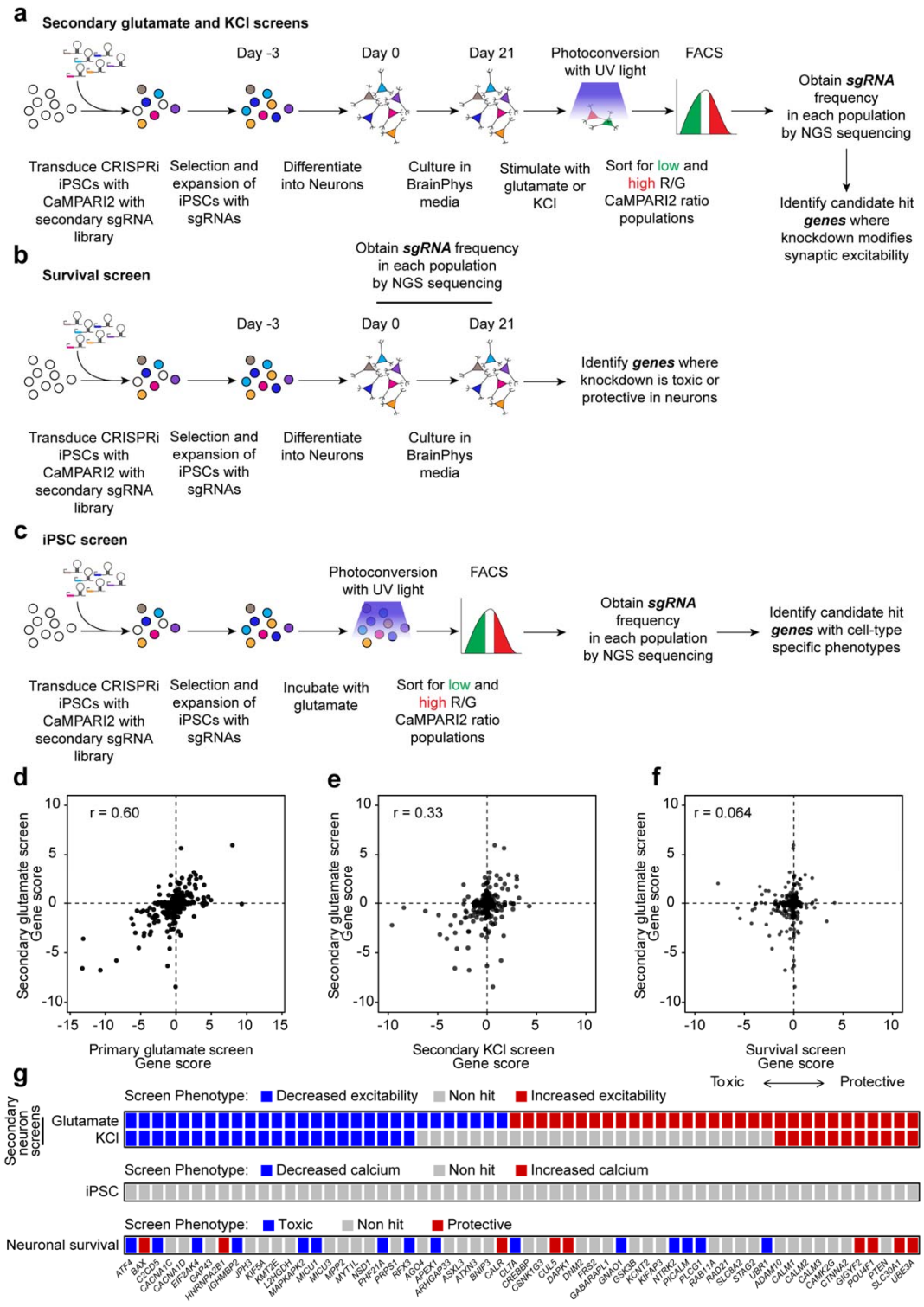

Figure 4. Secondary CRISPRi screens reveal excitability phenotypes in iPSC neurons.

(a) Screening strategy. CRISPRi iPSCs were transduced with a pooled lentivirus sgRNA library consisting of hit genes from the primary screen (1622 sgRNAs

targeting 424 genes). Exposure to puromycin selects for iPSCs successfully transduced with sgRNA construct. iPSCs were then differentiated into neurons via overexpression of NGN2 and cultured for 21 days. Neurons were then incubated with either 30 µM glutamate or 50 mM KCl, illuminated with UV light, and then separated by FACS into high and low red/green fluorescence ratio populations.

(b) Survival of neurons was assessed by comparing sgRNA frequency in neurons at the start of differentiation (day 0) and after 21 days of differentiation.

(c) Additionally, iPSCs expressing sgRNAs were treated with 30 µM glutamate for 5 minutes, illuminated with UV light, and then separated by FACS into high and low red/green fluorescence ratio populations. Frequency of cells expressing sgRNAs was determined by next-generation sequencing for high and low red/green ratio neuronal populations.

(d) Comparison of gene scores across different screens. Gene scores of knockdowns in both the primary and secondary screens with glutamate stimulation show a positive correlation (Pearson's R = 0.60).

(e) Many hit genes show a similar response to depolarization with KCl compared to stimulation with glutamate (Pearson's R = 0.33).

(f) Comparison of survival gene scores does not show a strong correlation (Pearson's R = 0.064) with gene score from glutamate stimulation.

(g) Heatmap of the top 30 hit genes that increase (positive hit) and decrease (negative hit) excitability in the glutamate stimulated screen. The KCl and glutamate screen share many hits, and none of the hit genes in the CaMPARI2 screens in neurons cross the FDR threshold when screened in iPSCs under the same conditions.

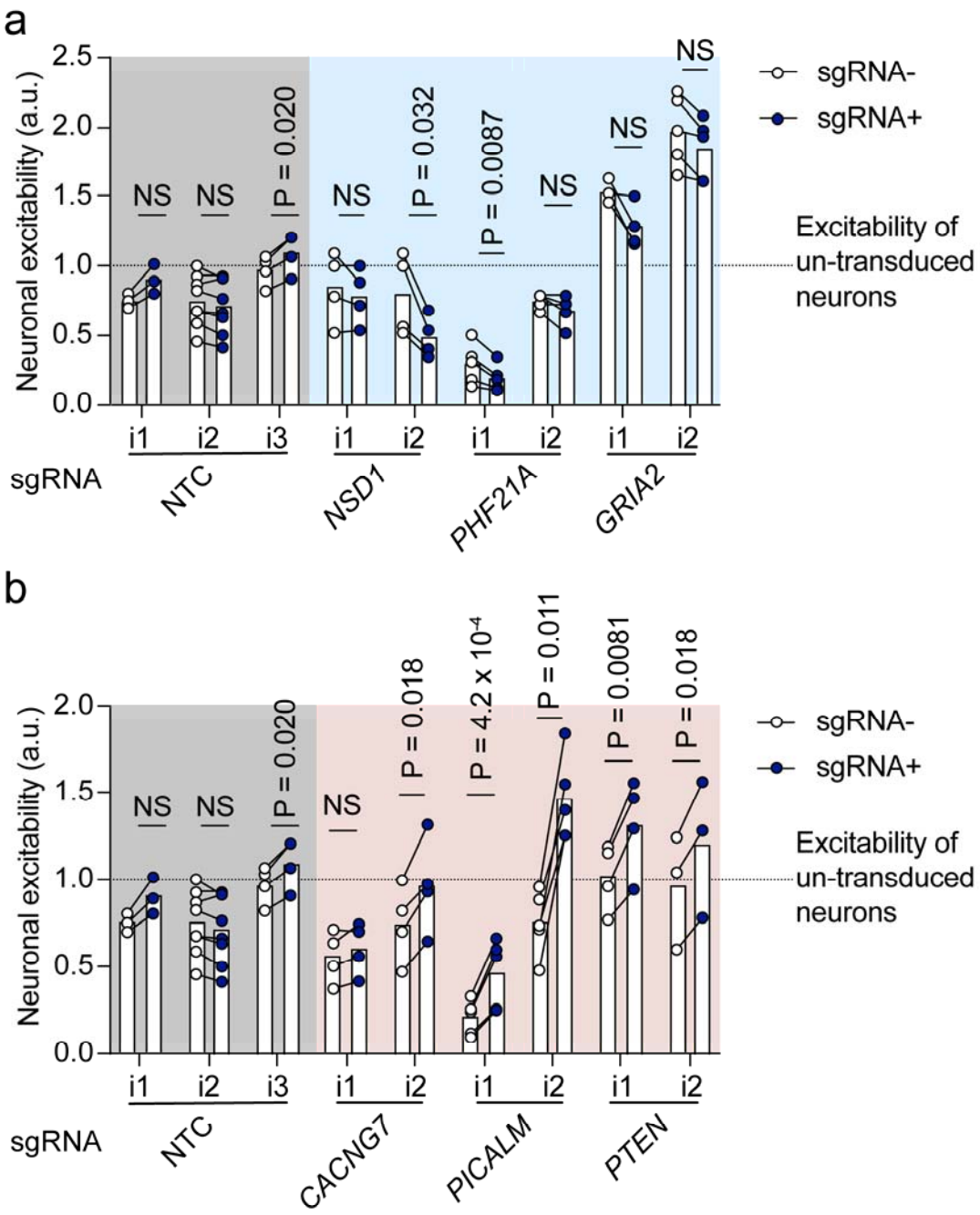

Figure 5. Flow validation of disease-associated excitability hit genes.

(a) CaMPARI2 neurons expressing sgRNAs targeting genes that, when knocked down, reduced neuronal excitability in response to glutamate stimulation in the secondary screens. This effect is observed intra-well, where sgRNA-containing neurons have a lower CaMPARI2 ratio than those that did not receive a sgRNA. Non-targeting controls (NTCs) are the same as in Figure 3A. Paired ratio t-test

made between neuron populations receiving sgRNA (sgRNA+) and not receiving guide (sgRNA-). N = 3-6 independent culture wells per measurement. Each individual experiment was normalized to the excitability (CaMPARI2 response) of wells where neurons did not receive a sgRNA. For intra-well comparisons, a paired ratio t-test between sgRNA- and sgRNA+ populations were performed for each sgRNA. The calculated P values were corrected for multiple hypotheses (Holm-Šídák method).

(b) CaMPARI2 neurons expressing sgRNAs targeting genes that, when knocked down, increased neuronal excitability in response to glutamate stimulation in the secondary screens. This effect is observed intra-well, where sgRNA containing neurons have a higher CaMPARI2 ratio than those that do not receive a sgRNA. Non-targeting controls (NTCs) are the same as in Figure 3A and Figure 5A . Paired ratio t-test made between neuron populations receiving sgRNA (sgRNA+) and not receiving guide (sgRNA-). N = 3-6 independent culture wells per measurement. Each individual experiment was normalized to the excitability (CaMPARI2 response) of wells where neurons did not receive a sgRNA. For intra-well comparisons, a paired ratio t-test between sgRNA- and sgRNA+ populations were performed for each sgRNA. The calculated P values were corrected for multiple hypotheses (Holm-Šídák method).

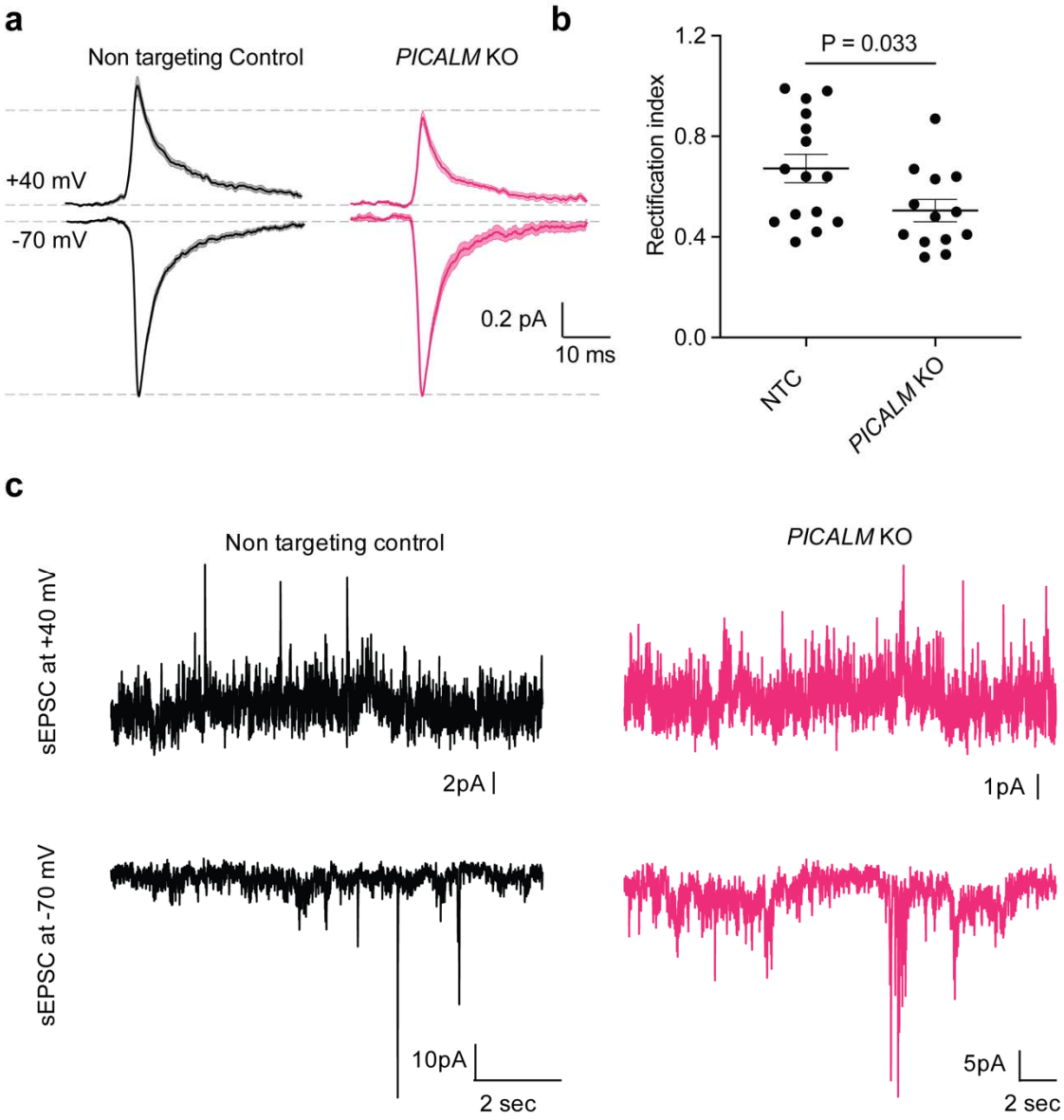

Figure 6. PICALM KO neurons have increase expression of calcium-permeable AMPA receptors.

(a) *PICALM* KOs exhibit a reduced rectification index (the ratio of current magnitude at +40 mV vs -70 mV) relative to NTC, suggesting an increased presence of synaptic calcium permeable AMPA receptors. The traces represent the mean and standard error of all sEPSC recordings from NTC and *PICALM* KO iNeurons and are shown normalized to the average -70 mV sEPSC for each neuron. (N = 15 NTC, 13 *PICALM* KO).

(b) PICALM KOs displayed a decreased rectification index as compared to NTCs (N = 15 and 13 neurons for NTCs and *PICALM* KOs, respectively; analyzed using the Mann-Whitney test). Error bars donate standard error.

(c) Sample sEPSC recordings from representative NTC and PICALM KO iNeurons.

Extended Data

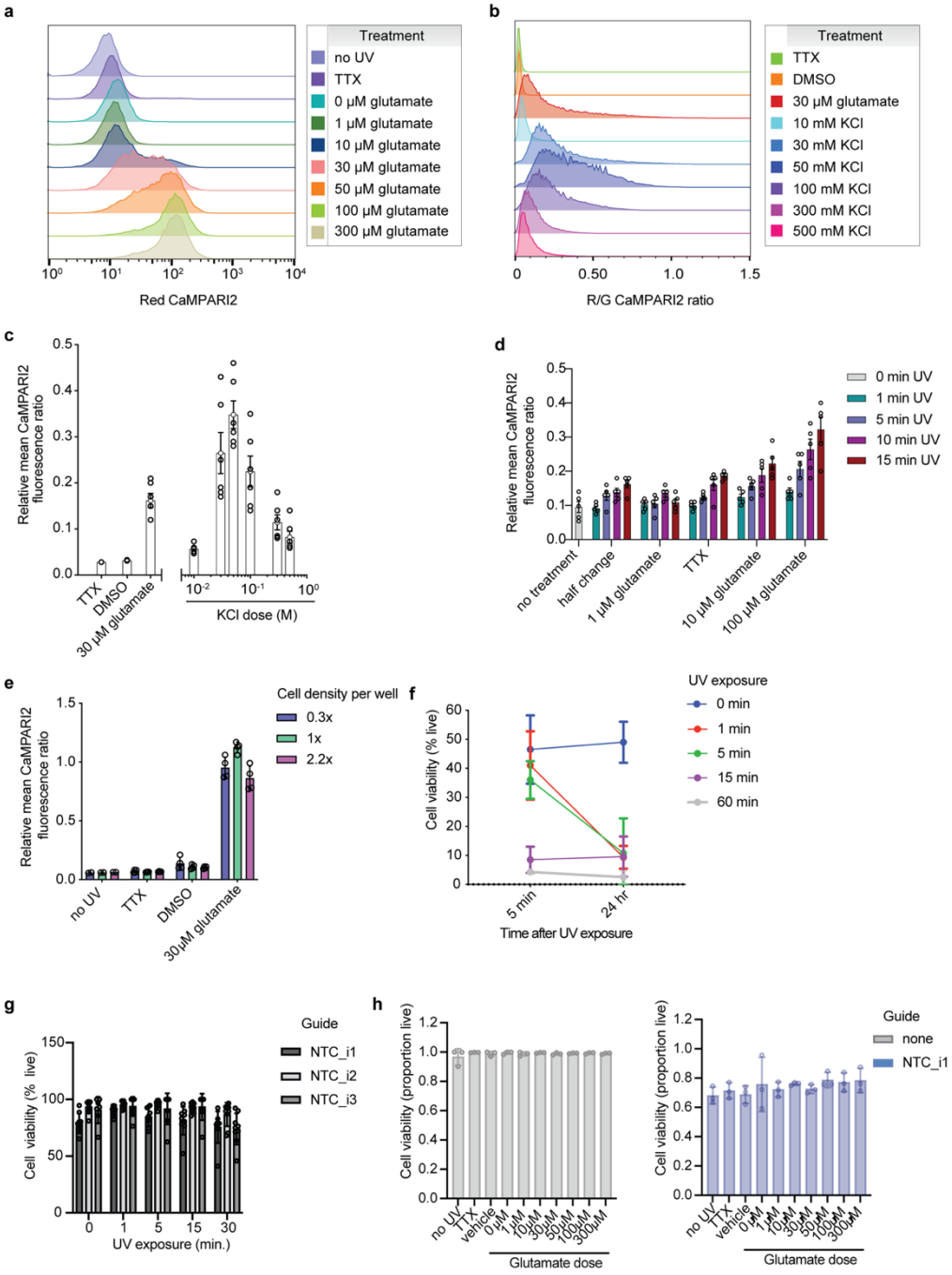

Extended Data Figure 1. CaMPARI reliably conveys AMPAR activation at the synapse without significant UV toxicity.

(a) CaMPARI dose response to glutamate. CaMPARI2 iNeurons were treated with TTX or various concentrations of glutamate (0, 1, 10, 30, 60, or 100 µM) and

illuminated with UV to measure photoconversion of CaMPARI2. Photoconversion increased in a dose-dependent manner.

(b) CaMPARI dose response to KCl. CaMPARI2 iNeurons were treated with TTX, 30 µM glutamate, 0.1% DMSO or various concentrations of KCl (10, 30, 50, 100, 300, 500 mM) and illuminated with UV to measure photoconversion of CaMPARI2. Photoconversion increased in a dose-dependent manner to a peak at 50 mM, where a decline in photoconversion was observed at higher concentrations of KCl.

(c) Quantification of CaMPARI2 red/green fluorescence ratio from (b). A non-linear fit could not be established, however the 50 mM KCl treatment was selected for later experiments due to the high conversion and range of response.

(d) CaMPARI photoconversion in response to various UV durations. CaMPARI2 iNeurons were treated with TTX or various concentrations of glutamate (0, 1, 10, or 100 µM) and illuminated with UV for various durations of time (0, 1, 5, 10, or 15 min). After illumination, cells were dissociated for flow cytometry and analyzed. N=5 independent culture wells.

(e) Measuring effect of cell density on CaMPARI photoconversion. Significant deviations from optimal plating conditions had no significant effects on photoconversion upon TTX, vehicle, or glutamate treatment. N=4 independent culture wells.

(f) Measuring UV toxicity in CaMPARI iNeurons. iNeurons were illuminated with UV for 0, 1, 5, 15, or 60 minutes and stained with Trypan Blue or TOPRO viability stain 5 minutes or 24 hour later to assess UV toxicity. N=3 independent culture wells.

(g) Measuring UV toxicity in CaMPARI iNeurons. CaMPARI iNeurons were illuminated with UV for 0, 1, 5, 15, or 30 minutes. To perform viability staining with TO-PRO-3 (ThermoFisher T3605), cells were washed 3x with DPBS, stained with TO-PRO-3 diluted 1:1000 in DPBS and DAPI counterstain for 30 minutes at room temperature. After staining, cells were washed 3x with DPBS and imaged on ImageXpress. Images were analyzed using CellProfiler analysis software and thresholding was done to determine the proportion of viable cells per well. N=9 independent culture wells.

(h) Measuring glutamate toxicity. CaMPARI iNeurons were treated with 0, 1, 3, 10, 30, 50, 100, µM of glutamate for 5 minutes and UV illuminated for 5 minutes. TO-PRO-3 staining was performed to measure acute glutamate treatment toxicity. N=3 independent culture wells.

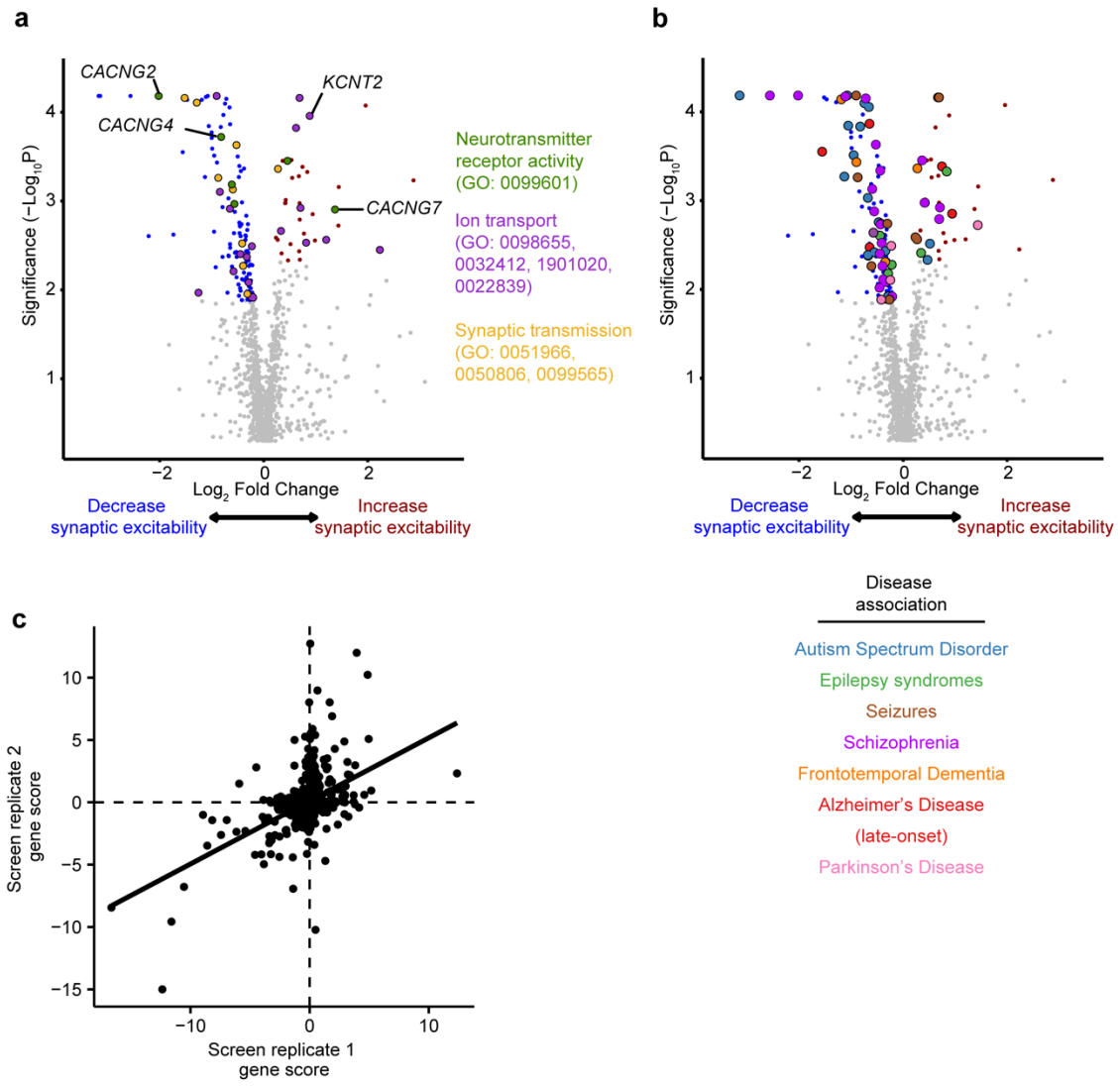

Extended Data Figure 2. Results from Primary screen

(a) Volcano plot summarizing the effect of knockdowns on CaMPARI phenotypes and the determine statistical significance for targeted genes (Mann-Whitney U test). Dashed lines indicate a false-discovery rate (FDR) cutoff of 0.05, based on the phenotype score for gene calculated from 5 targeting sgRNAs. Black points indicate hit genes where knockdown changes CaMPARI red/green fluorescence ratio in response to glutamate stimulation, while grey points indicate non-hits. Genes related to synaptic transmission (purple) and ion transport (orange) are highlighted based on Gene Ontology terms.

(b) Disease associated genes from DisGenNet and whole-exome sequencing (Satterstrom et al)[9] overlap with hit genes from CaMPARI screen.

(c) Scatterplot of gene scores from each replicate of the primary screen shown the correlation between screens. Pearson's R = 0.49, linear regression fit depicted by solid black line.

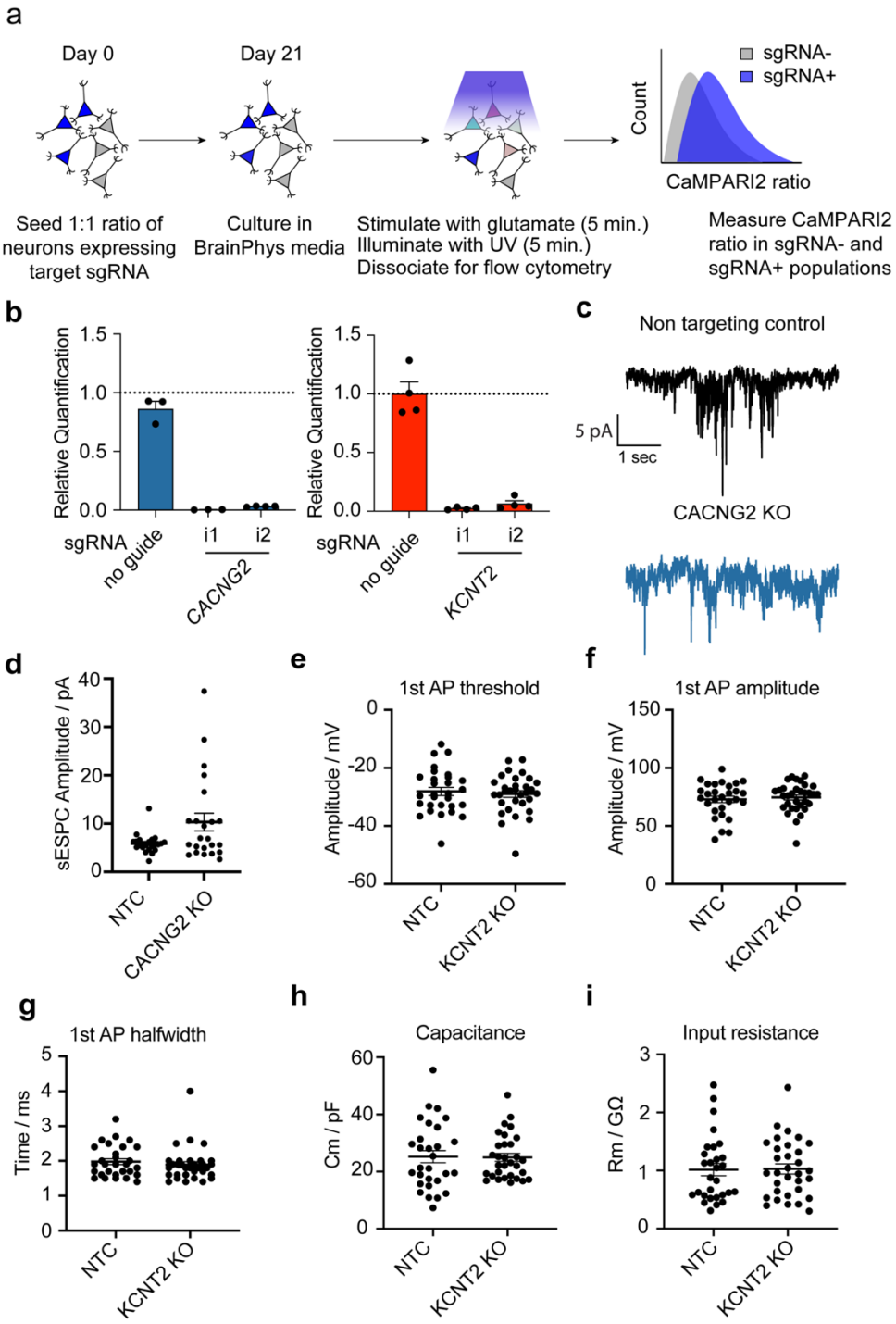

Extended Data Figure 3. Electrophysiology profiles of iNeurons with *KCNT2* and *CACNG2* knockdowns.

(a) Schematic of intra-well comparison experiments with 50% of CaMPARI2 iNeurons expressing a sgRNA for a target gene. A 1:1 ratio of iNeurons expressing the sgRNA: not expressing a sgRNA are seeded and differentiated. These are then treated with the same glutamate and photoconversion conditions.

These are gated based on the presence of BFP in the sgRNA construct, and the CaMPARI2 ratio is directly compared between the two populations.

(b) RT-qPCR shows the knock down efficiency of the sgRNAs targeting *CACNG2* (blue) and *KCNT2* (red). N = 4 biological replicates per condition. Error bars are SEM.

(c) Sample sEPSC recordings from NTC (black trace) and *CACNG2* KO (blue trace) iNeurons

(d) CACNG2 KO iNeurons show a slight increase in sESPC amplitude that is not statistically significant. (NTC: 22 neurons, CACNG2 KO:23 neurons, Mann-Whitney test .

(e-i) No differences between NTCs (N= 29 neurons) and KNCT2 KOs (N = 32 neurons) in either passive membrane properties or action potential kinetics. Error bars donate standard error.

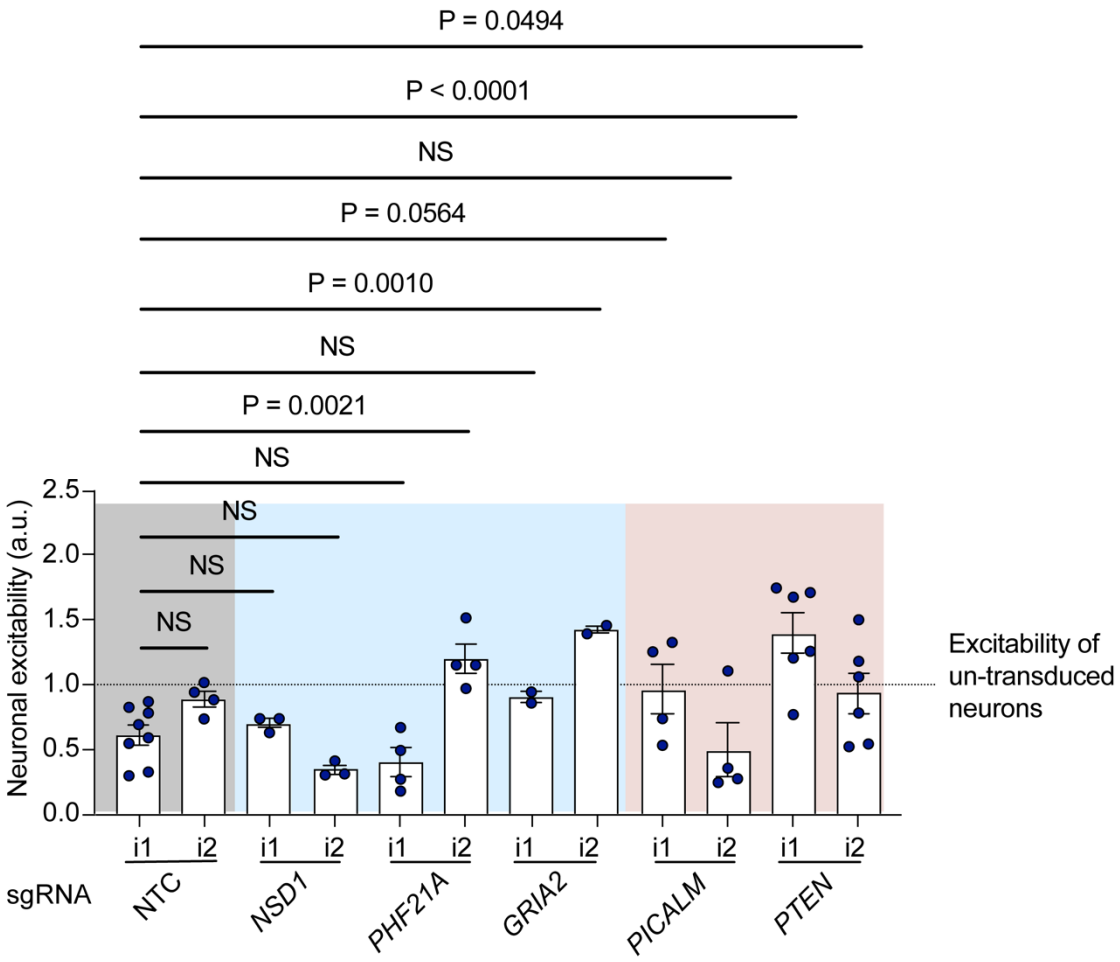

Extended Data Figure 4. Validation of KDs from secondary screens

In cultures where 100% of CaMPARI2 iNeurons are expressing sgRNAs targeting *NSD1* and *PHF21A,* these iNeurons lack statistically significant reduced neuronal excitability in response to glutamate stimulation observed in the screen relative to non-targeting controls. iNeurons expressing sgRNAs targeting *PTEN* show the expected increase in activity. For iNeurons expressing sgRNAs targeting *GRIA2* and *PICALM*, the expected screen phenotype is not preserved when 100% of the cells have the knockdown. CaMPARI2 ratios are normalized to neuron samples that do not receive a sgRNA and are run on the flow cytometer on the same day. N = 2-8 independent culture wells per experiment. Each individual experiment was normalized to the excitability (CaMPARI2 response) of wells where neurons did not receive a sgRNA. Error bars denote standard error. P values calculated by ANOVA, using NTC_i1 as reference. P > 0.05 = not significant (NS).

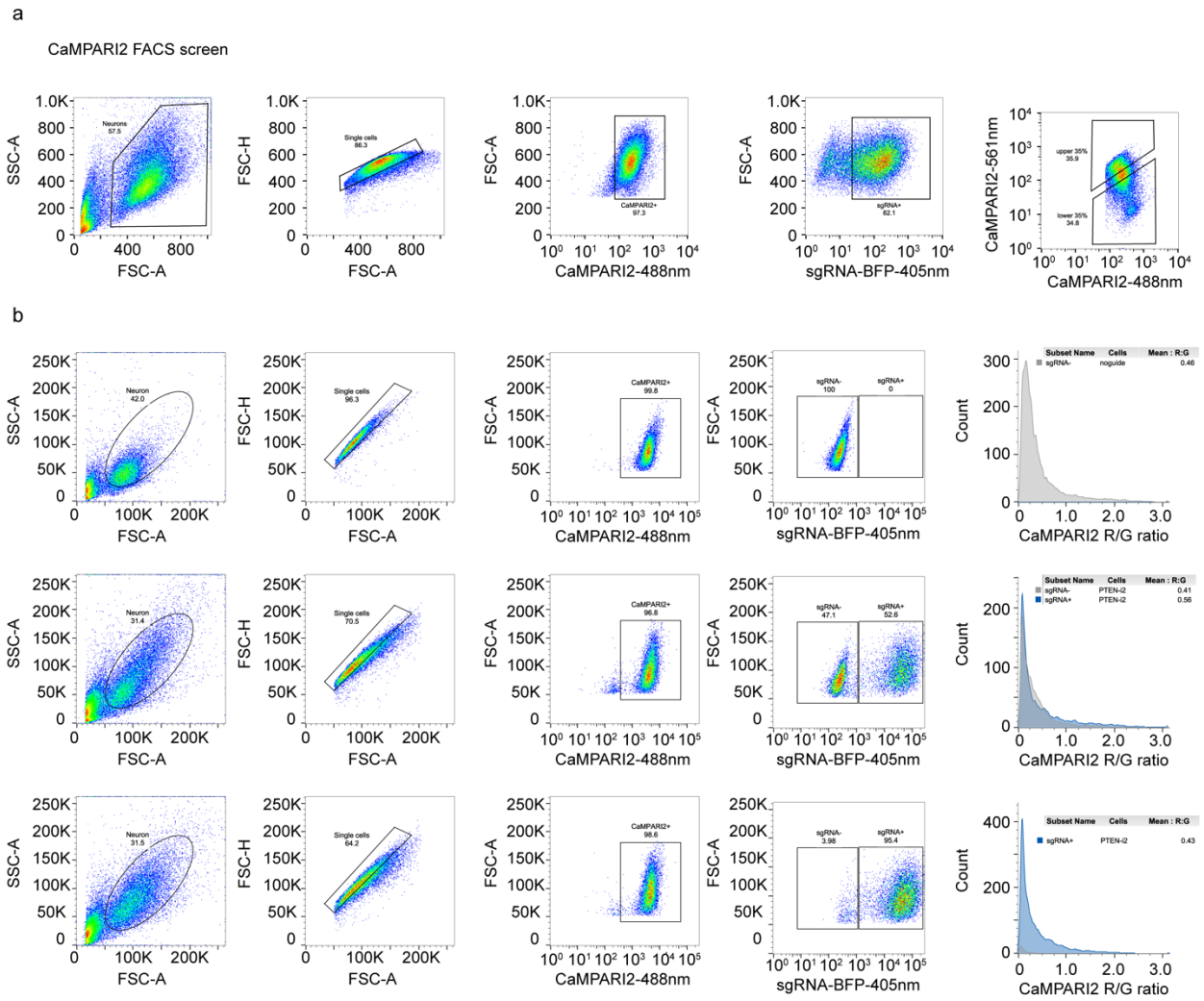

Supplementary Figure 1. Gating strategies for FACS-based screens and for CaMPARI2 ratio validation experiments.

a,b. Gating strategies for (a) CaMPARI2 screen and (b) CaMPARI2 flow cytometry analysis of neuronal excitability. Intact iPSC-neurons were identified from FSC-SSC plot and then gated for singlets. These cells were then gated for CaMPARI2 and BFP (sgRNA) expression. For FACS screen (a) these cells were then sorted into high and low CaMPARI2 ratio populations corresponding with the top 35% and bottom 35% of the signal distribution. (b) For flow analysis, the mean CaMPARI 2 R/G ratio was measured for BFP- (sgRNA-) and BFP+ (sgRNA+) cells.